Effective high-throughput RT-qPCR screening for SARS-CoV-2 infections in children

Felix Dewald[1,2]*, Isabelle Suárez[2,3,4]*, Ronja Johnen[5], Jan Grossbach[5], Roberto Moran-Tovar[6], Gertrud Steger[1], Alexander Joachim[7], Gibran Horemheb Rubio[1], Mira Fries[3,8], Florian Behr[3,8], Joao Kley[3], Andreas Lingnau[9], Alina Kretschmer[3], Carina Gude[5], Guadelupe Beazes-Flores[10], David Laveaga del Valle[10], Alberto Roblero-Hernandez[10], Jesus Magana-Cerino[10], Adriana Torres Hernandez[11], Jesus Ruiz-Quinones[10], Konstantin Schega[8], Viktoria Linne[3], Lena Junker[3], Marie Wunsch[1], Eva Heger[1], Elena Knops[1], Veronica Di Cristanziano[1], Meike Meyer[7], Christoph Hünseler[7], Lutz T. Weber[7], Jan-Christoffer Lüers[12], Gustav Quade[13], Hilmar Wisplinghoff[14], Carsten Tiemann[15], Rainer Zotz[16], Hassan Jomaa[17], Arthur Pranada[18], Ileana Herzum[19], Paul Cullen[20], Franz-Josef Schmitz[21], Paul Philipsen[22], Georg Kirchner[23], Cornelius Knabbe[24], Martin Hellmich[25], Michael Buess[8], Anna Wolff[8], Annelene Kossow[8,26], Johannes Niessen[8], Sebastian Jeworutzki[27], Jörg-Peter Schräpler[27], Michael Lässig[6], Jörg Dötsch[7], Gerd Fätkenheuer[2,3], Rolf Kaiser[1], Andreas Beyer[5]*, Jan Rybniker[2,3,4]*, Florian Klein[1,2,4]*

Affiliations

1. Institute of Virology, Faculty of Medicine, University Hospital Cologne, University of Cologne, Cologne, Germany
2. Center for Molecular Medicine Cologne, University of Cologne, Cologne, Germany.
3. Department I of Internal Medicine, Division of Infectious Diseases, Faculty of Medicine, University Hospital Cologne, University of Cologne, Cologne
4. German Center for Infection Research, Partner Site Bonn-Cologne, Cologne, Germany
5. CECAD Research center, University of Cologne, Cologne, Germany
6. Institute for Biological Physics, University of Cologne, Cologne, Germany
7. Department of Pediatrics, Faculty of Medicine, University Hospital Cologne, University of Cologne, Cologne, Germany
8. Health department of Cologne, Cologne, Germany
9. Ministry of Schools and Education of North Rhine-Westphalia, Düsseldorf, Germany
10. Centro de Investigación en Enfermedades Tropicales y Emergentes, Hospital Regional de Alta Especialidad, Dr. Juan Graham Casasús, Villahermosa, Mexico
11. Bioclilab SA de CV, Villahermosa, Mexico
12. Department of Otorhinolaryngology, Head and Neck Surgery, Faculty of Medicine, University Hospital Cologne, University of Cologne, Cologne
13. MVZ Labor Dr. Quade & Kollegen GmbH, Cologne, Germany

14. Labor Dr. Wisplinghoff, Cologne, Germany

15. Labor Krone, Bad Salzuflen, Germany

16. Labor ZotzKlimas, Düsseldorf, Germany

17. Synlab, Leverkusen, Germany

18. Medizinisches Versorgungszentrum Dr. Eberhard & Partner, Dortmund, Germany

19. Medizinische Laboratorien Düsseldorf, Düsseldorf, Germany

20. MVZ Labor Münster, Münster, Germany

21. Mühlenkreiskliniken, Minden, Germany

22. Labor Mönchengladbach MVZ Dr. Stein und Kollegen, Mönchengladbach, Germany

23. Eurofins Laborbetriebsgesellschaft Gelsenkirchen GmbH & Eurofins MVZ Medizinisches Labor Gelsenkirchen GmbH, Gelsenkirchen, Germany

24. Heart- and Diabetes Center NRW, Medical Faculty, Ruhr-University Bochum, Institute for Laboratory and Transfusion Medicine, Bochum, Germany

25. Institute of Medical Statistics and Computational Biology, Faculty of Medicine, University Hospital Cologne, University of Cologne, Cologne

26. Institute for Hygiene, University Hospital Münster, Münster, Germany

27. Faculty of Social Science, Ruhr-University Bochum, Bochum, Germany

* contributed equally to this manuscript

Abstract

Systematic SARS-CoV-2 testing is a valuable tool for infection control and surveillance. However, broad application of high sensitive RT-qPCR testing in children is often hampered due to unpleasant sample collection, limited RT-qPCR capacities and high costs. Here, we developed a high-throughput approach ('Lolli-Method') for SARS-CoV-2 detection in children, combining non-invasive sample collection with an RT-qPCR-pool testing strategy. SARS-CoV-2 infections were diagnosed with sensitivities of 100% and 93.9% when viral loads were $>10^6$ copies/ml and $>10^3$ copies/ml in corresponding Naso-/Oropharyngeal-swabs, respectively. For effective application of the Lolli-Method in schools and daycare facilities, SEIR-modeling indicated a preferred frequency of two tests per week. The developed test strategy was implemented in 3,700 schools and 698 daycare facilities in Germany, screening over 800,000 individuals twice per week. In a period of 3 months, 6,364 pool-RT-qPCRs tested positive (0.64%), ranging from 0.05% to 2.61% per week. Notably, infections correlated with local SARS-CoV-2 incidences and with a school social deprivation index. Moreover, in comparison with the alpha variant, statistical modeling revealed a 36.8% increase for multiple (≥2 children) infections per class following infections with the delta variant. We conclude that the Lolli-Method is a powerful tool for SARS-CoV-2 surveillance and infection control in schools and daycare.

Introduction

The clinical course of COVID-19 in children is generally mild[1,2]. However, severe courses, deaths, and post-acute COVID-19 syndrome have been described and pose a risk to children when exposed to SARS-CoV-2[3,4]. Moreover, viral loads measured in infected children can be as high as those in adults[5], which is consistent with the transmission of SARS-CoV-2 among children and from children to adults[6]. In order to

control SARS-CoV-2 infections, schools have been closed worldwide, resulting in the loss of approximately 50% of all school lessons in 2020[7]. However, while school closures can reduce SARS-CoV-2 transmissions when imbedded in a general lock-down strategy, the negative impact on the development and health of children is substantial and is manifested by e.g. higher rates of reduced emotional well-being, severe eating disorders, and overt psychiatric disease[8–10].

Early detection of SARS-CoV-2 infections can contribute to infection control[11]. In addition, SARS-CoV-2 surveillance in schools allows to determine the efficiency of non-pharmaceutical interventions (NPIs)[12]. Therefore, several test strategies for schools and daycare facilities have been developed. In these, samples were mostly obtained by self-sampling using rapid antigen detection tests (RADTs) or RT-qPCR analyses[13–16]. However, various challenges remain including reduced sensitivity of RADTs[17], acceptance of specimen collection by children[18], and limited RT-qPCR capacities[19]. Despite the recent authorization for SARS-CoV-2 vaccines in children aged 5-11 years[20], effective and sound test strategies remain critical to ensure infection control in open schools and daycare facilities. This is particularly important considering the dynamic situation of the SARS-CoV-2 pandemic in which new variants of concerns (VOCs) emerge and spread[21]. Here, we developed a non-invasive sampling approach combined with high-throughput pooled RT-qPCR testing (Lolli-Method) followed by the design of a test concept for schools and daycare facilities. This test concept was successfully implemented as a SARS-CoV-2 screening program for over 800,000 children and demonstrated a precise monitoring and early detection of SARS-CoV-2 infections.

Results

Developing the Lolli-Method to screen for SARS-CoV-2 infections in children

A widely applicable SARS-CoV-2 screening in children requires the combination of i.) an easy, safe and non-invasive sampling method with ii.) a resource-saving, reliable and scalable SARS-CoV-2 testing method. To meet these requirements, we developed the Lolli-Method by which a regular swab is used for self-sampling, i.e. to be sucked on for 30 seconds (Lolli-swab), combined with a pooled RT-qPCR analysis. In order to determine the sensitivity of this method, we investigated 254 acutely infected individuals in a side-by-side sampling approach using Nasopharyngeal-/Oropharyngeal (Np-/Op) versus Lolli-swab. Lolli-swabs were collected under supervision and all samples were analyzed by RT-qPCR (Fig. 1a, Supplementary Fig. 1). By using the Lolli-Method, 95 out of 118 infected individuals were detected when sampled in the morning and 101 out of 153 when sampled during the day. Detected viral loads obtained by the Lolli-Method were lower (geometric mean 2.22×10^3 copies/ml) than viral loads measured in Np-/Op-swabs (geometric mean 6.36×10^4 copies/ml, $p<0.0001$, Fig. 1b and 1c, Supplementary Data 1). However, while Lolli-swabs showed only 50% sensitivity in samples with corresponding viral loads of $<10^3$ copies/ml, diagnostic sensitivities of 91.4% and 100% were reached for matched Np-/Op-swabs with viral loads of 10^3-10^6 and $>10^6$ copies/ml, respectively (Figure 1d). Next, we determined the impact on the sensitivity by having food and liquid intake one hour before sampling (Fig. 1e, Supplementary Data 2), the use of different swab-types (Fig. 1f, Supplementary Data 3) and the dilution effect by the pooling-process (Fig. 1g, Supplementary Data 4). While different swab-types had no effect on sensitivity, breakfast one hour before sampling and pooling of up to 100 Lolli-swabs reduced the detected viral load by 2.2- and 3.3-fold, respectively. However, these differences did not result in a relevant reduction of overall sensitivity, detecting 56 out of 57 samples

despite breakfast or pooling. Finally, specificity of the Lolli-Method was found to be 100%, testing 55 healthy individuals individually with Np-/Op-and Lolli-swabs (Supplementary Data 5).

We concluded that the Lolli-Method is an easy and non-invasive method that is highly sensitive in detecting infected individuals with viral loads above 10^3 copies/ml.

High-throughput Lolli-Method screening concept in children

Next, a screening concept for schools and daycare was developed. As part of this concept, Lolli-swabs of one class or group were obtained and pooled at sampling-site, followed by RT-qPCR analysis. To this end, each child of a class received a Lolli-swab, performed self-sampling and placed it in a common 50 ml tube (Fig. 1h). Very young children or children with disabilities received assistance by their parents or teachers. The pooled samples were tested by SARS-CoV-2 RT-qPCR. In case the pool was tested negative, all children were assumed to be SARS-CoV-2 negative. In case the pool was tested positive, children of the positive pool were re-tested individually in order to identify the infected individuals (Fig. 1h).

To determine an optimal test-frequency, the efficiency of a long-term SARS-CoV-2 screening was estimated using an SEIR-model (Fig. 1i and 1j, Supplementary Table 1). Simulations of 8-week-test-periods were carried out for fully-connected populations of 20 individuals, performing ensemble averages of over 10^4 runs. Simulations were performed for different basic reproduction values (R_0) of SARS-CoV-2 and different scenarios of SARS-CoV-2 prevalence in the general population (0.01% and 0.1%). The total number of infected individuals, the number of infections due to transmissions within the test-population and the number of infections detected by the screening were calculated for different test-frequencies (0, 1, 2 or 3 times per week) with a turn-around time of 1 day and mandatory quarantine of 14 days for all 20

individuals (See methods). As a result, the proportion of prevented transmissions was 36-66%, 46-77%, and 53-82% for testing 1, 2, or 3 times per week, respectively (Fig. 1k). Taking logistics and limited RT-qPCR capacities into account, a test-frequency of twice per week was considered most effective and was used for the subsequent implementation of a screening program.

Implementing the Lolli-Method screening concept in schools and daycare

The Lolli-Method screening concept was implemented as part of a governmental SARS-CoV-2 testing program in 3,700 elementary schools and special needs schools in North Rhine-Westphalia, Germany, testing 742,771 students twice a week (Fig. 2a, Supplementary Table 2). Testing was mandatory for all students. Students had a median age of 8 years (IQR 2 years) with 354,125 (47.69%) being female and 388,646 (52.32%) being male. On average, 21.1 students were registered per class and 197.3 students per school (Fig. 2b). Sampling was conducted from calendar week 19 to 37 in 2021, which included 8 weeks before (calendar week 19-26) and 5 weeks after (calendar week 33-37) the summer holidays. During this period, the 7-day incidence in North Rhine-Westphalia ranged from 14.4 to 146.7 with a maximum in calendar week 34 (Fig. 2c). Notably, while at the beginning the variant of concern (VOC) alpha was predominant, the delta variant accounted for the majority of cases starting with calendar week 26 (Fig. 2c).

For the 3,700 schools that were located within an area of 34,098 km^2, sample transport as well as RT-qPCRs were performed by 12 diagnostic laboratories (Supplementary Fig. 2, Supplementary Data 6). All RT-qPCR results were reported to a central database and data was checked for plausibility and invalid items were removed (Supplementary Fig. 3). In total, 1,110,033 RT-qPCRs were carried out (983,941 pool-and 126,092 single-RT-qPCRs). Average pool-size was 10.2 and 16.7

Lolli-swabs/pool during calendar weeks 19-21 and 22-26/33-37, respectively, estimating an overall SARS-CoV-2 testing of 16,943,470 swabs within a time period of 13 weeks (Fig. 2d). Mean turn-around time for processing of pool-RT-qPCRs was 7.59 hours and 9.14 hours for single-RT-qPCRs (Supplementary Fig. 4). 96.2% of all pool-RT-qPCR results were communicated before 6:00 a.m. on the next day (Supplementary Data 6). In addition, the Lolli-Method was applied to 698 daycare facilities in the city of Cologne, testing approximately 48,149 children within the age of 1 to 6 years and 13,577 staff members twice per week for a period of 6 months (Supplementary Fig. 4). Both in schools and daycare facilities, the program was well accepted and continued beyond the reported time period.

We concluded that the Lolli-Method can be applied to educational settings including daycare facilities for high-throughput testing of SARS-CoV-2 infections.

Monitoring SARS-CoV-2 infections in schools

In total, 6,364 of 983,941 pool-RT-qPCRs in schools tested positive (0.65%). 1,316 pool-RT-qPCRs tested positive before (calendar week 19-26), while 5,048 tested positive after the summer holidays (calendar week 33-37) (Fig. 3a). The rate of positivity of pool-RT-qPCRs was 0.46% in calendar week 19 and decreased continuously to 0.05% in calendar week 26. After the summer holidays, rate of positivity decreased from 2.61% in calendar week 33 to 0.92% in calendar week 37 (Fig. 3b). The number of infected individuals per positive pool-RT-qPCR was estimated to be 1.3 on average (Supplementary Fig. 6). In order to determine the false-negative rate of the implemented Lolli-Method, we investigated all reported index-cases of children attending elementary schools in the city of Cologne from calendar week 19 to 36 (n=653, Supplementary Fig. 7). To this end, contact-tracing information was obtained by the local health authorities on 569 from 653 index-cases (87.1%). When excluding

index-cases that were not tested by the Lolli-Method within 72h before their positive test, detection rate of the Lolli-Method of confirmed index-cases was 89.1% (Supplementary Fig. 7), indicating a reliable detection of SARS-CoV-2 infections in children. Furthermore, we confirmed the effect of the sample dilution by the pooling procedure described in the validation of the Lolli-Method (Figure 1g) by comparing the Ct-values of the pool-RT-qPCRs and the corresponding single-RT-qPCRs (mean Ct-values 30.07 vs. 32.3, $p<0.0001$, Wilcoxon-matched-pairs signed rank test; Supplementary Fig. 8)

SARS-CoV-2 7-day pool-incidence (= number of positive pool-RT-qPCRs/100.000 tested children in 7 days, see Methods, also for determination of number of samples per pool-RT-qPCR) varied among districts from 0 to 416.2 (Fig. 3c) and correlated with SARS-CoV-2 incidence of the general population within a district ($r=0.76$, $p<0.0001$; Fig. 3d). Of 3,700 participating schools, 3,648 were tested before and after the summer holidays. Of those, 2,315 (63.46%) schools were found to have at least one positive pool-RT-qPCR result, with numbers of positive pool-qPCRs per school ranging from 1 (22.2%), 2 (15.8%) and 3 (9.5%) to a maximum of 22 (0.03%, Fig. 3e).

Moreover, we investigated potential associations of SARS-CoV-2 infections in schools with grade levels, type of school, population density and socioeconomic status (SES) quantified using a school social deprivation index (SSDI)[22]. This index had been generated using a confirmatory factor analysis in which schools were assigned to social deprivation levels on a scale from 1 to 9 with 1 reflecting the highest SES and 9 the lowest. While no association between infections and grade levels or type of school was found, a moderate correlation for population density ($r=0.56$, $p<0.0001$) was detected. Moreover, the SSDI strongly correlated with the average number of positive pool-RT-qPCRs per student and per school ($r=0.99$, $p<0.0001$) (Fig. 3f and 3g).

We concluded that the Lolli-Method is capable of reliably detecting SARS-CoV-2 infections in schools and is a valuable tool to determine factors associated with SARS-CoV-2 infections in schools.

High-throughput screening reveals differences in infection dynamics for SARS-CoV-2 variants in schools

Based on molecular surveillance data published by the German public health institute (Robert Koch Institute) (Fig. 2c), we estimated the fraction of positive pool-RT-qPCRs assigned to the alpha variant (B.1.1.7) to be 92.9% before the summer holidays while 99.54% were assigned to the delta variant (B.1.167.2) after the summer holidays (Fig. 4a). Mean Cycle threshold (Ct)-values of positive pool-RT-qPCRs decreased significantly after the summer holidays, with an average Ct-value of 33.61 before (alpha variant) and 32.55 after (delta variant) the summer holidays ($p<0.0001$, Mann-Whitney test). While the overall difference was small (1.06 Ct-values), pool-RT-qPCRs tested positive with high viral loads (Ct-value≤25) were observed 3.1-fold more often for the delta variant compared to the alpha variant (Fig. 4b and 4c). Moreover, for viral loads detected with Ct-values ≤20, the difference between alpha and delta was even 7.6-fold.

In order to estimate a possible effect of the increase in pool-RT-qPCRs with low Ct-values on infection dynamics, the increase in positive pool-RT-qPCRs containing more than one infected child was statistically modeled, using data from calendar weeks 19-25 (alpha period) and calendar weeks 34-37 (delta period). The numbers of infected children per positive pool-RT-qPCRs expected by chance and without in-class transmissions (Null model) were estimated, while controlling for local incidence rates and the SSDI, and compared to the observed number (Methods and Supplementary Fig. 9). During alpha- and delta periods, numbers of positive pool-RT-qPCRs

containing more than one infected child were 13 and 79, respectively, while 14.27 and 63.4 were expected based on the Null model (Fig. 4e). The ratio between observed and expected frequencies of pool-RT-qPCRs containing more than one infected child was 0.9 for the alpha period and 1.25 for the delta period (Fig. 4f). This amounted to an increase of 36.8% in positive pool-RT-qPCRs containing more than one infected child during the delta period.

We concluded that, during the delta period, more children with higher viral loads were present in schools and that parameters changing infection dynamics can be detected by applying the Lolli-Method in schools.

Discussion

During the pandemic, schools have been frequently closed to reduce SARS-CoV-2 transmissions[23]. However, closure of schools and daycare facilities have had a substantial impact on development, physical and mental health of children[8–10,24]. Therefore, concepts are essential to support safe and open school settings. This is particularly important as new VOCs emerge that may substantially change infection dynamics.

Systematic testing can prevent transmissions in educational settings and gain insights of measures for infection control in children[14]. In addition, effective test strategies may allow to use NPIs more specifically and to reduce quarantine measures to keep school absence of children to a minimum[14]. Effective screening strategies require an easy and non-invasive sample collection, high sensitivity assays for early detection of infections, and high-throughput application[25]. As one SARS-CoV-2 test strategy, RADTs have been used[26]. While RADTs have the advantage of providing immediate test results, disadvantages include limited sensitivity[17], variation in specimen quality[27], and limited feasibility of self-sampling by young children. Finally, a

high acceptance was observed for sample collection based on the Lolli-Method as demonstrated in a previous study[28].

RT-qPCR-based approaches for SARS-CoV-2 screenings in schools have been described[15,29,30]. In these studies, different specimens, such as buccal and anal swabs as well as gargling solutions and saliva samples were obtained. Some of these sampling methods may cause difficulties, e.g. gargling solutions may increase the risk of viral transmission during sampling because of aerosol generation. Moreover, strategies that depend on sample-pooling in the diagnostic laboratory require significantly more capacities in comparison of processing Lolli-swabs that have already been pooled in schools[31,32]. Considering limited resources of RT-qPCR-capacities, the Lolli-Method can therefore be advantageous as demonstrated by our report in which less than 1.2 million RT-qPCRs were performed for investigating a total of 16.5 million swabs. However, high SARS-CoV-2 incidences yield larger numbers of positive pools associated with increasing numbers of follow-up single RT-qPCRs, which reduces the benefit of a pooling strategy and limit the application of pool-testing in high incidence settings[33].

There is an urgent medical need to determine the role and effect of NPIs in educational settings, such as school-closures[34], mandatory mask usage[35], and split-class lessons[36]. Notably, the described screening was sensitive enough to detect biological differences of the infection dynamics between the alpha and the delta variant[37]. Thus, the Lolli-Method may be further used to assess infection dynamics introduced by new variants[21] as well as determine the impact of measures taken in schools to prevent SARS-CoV-2 infections. Moreover, we could show a correlation between infection rates in schools and regional SARS-CoV-2 incidence which is in line with previous studies[16,38].

Limitations of our report include aspects of the data quality. These contain i) reporting of the viral load as non-standardized Ct-values and ii) incomplete reporting of pool-sizes. However, there is a high level of consistency and comparability of Ct-values since RT-qPCRs were performed by the same laboratories during the course of the screening. In addition, due to the obligation for students to participate in the screening program, we were able to estimate pool-sizes by extrapolation from reported data. One limitation of pool testing is that it is particularly suitable for low to medium SARS-CoV-2 incidences. For this reason, we consider it necessary to develop scalable modifications for the test concept for high-incidence phases (e.g. pool-size adjustment or additional use of RADTs). Finally, we do not provide real life effectiveness data of the Lolli-Method screening program in direct comparison with other screening programs (e.g. RADT settings). Therefore, further analyses are necessary to determine the effectiveness to reduce SARS-CoV-2 infections in children and the entire population using Lolli-testing in schools.

In summary, we developed, validated and implemented a non-invasive and sensitive technique for SARS-CoV-2 (self)-sampling that can be used for high-throughput application and screening. We consider this sampling method applicable to schools and daycare facilities providing a reliable tool for screening and surveillance of SARS-CoV-2 infections in children.

Methods

Ethical considerations

Prospective Validation of the Lolli-Method

The prospective validation study was approved by the Institutional Review Board (IRB) of the Faculty of Medicine and University Hospital of Cologne, Cologne, Germany (number 20-1405) as well as by the IRB of the High Specialty Regional, Villahermosa, Mexico (number 0130144). The participants were either study patients of the University Hospital Cologne, Germany or of the test center of the High Specialty Regional Hospital, Villahermosa, Tabasco, Mexico. All participants gave their written informed consent before the start of the study.

Retrospective analysis of the SARS-CoV-2 screening in schools

The retrospective analysis of the SARS-CoV-2 screening in schools by the University Hospital of Cologne was engaged by the Ministry of Education and Schools and approved by the IRB of the Faculty of Medicine, University Hospital of Cologne, Germany (number 21-1358). Since 10th of May 2021, under the direction of the Ministry of Schools and Education and as part of the governmental SARS-CoV-2 screening program “Lolli-Test NRW”, two Lolli-tests per week combined with a pooled RT-qPCR analysis were mandatory for all students at elementary schools and special needs schools in the state of North Rhine-Westphalia. Because testing was mandatory and in line with German law, no informed consent was required and obtained. 12 diagnostic laboratories were involved in processing the Lolli-swabs. These laboratories transmitted anonymized, de-identifiable data to a digital database (Medeora Köln GmbH) for quality assurance purposes. Data were transmitted for pool-RT-qPCRs and single RT-qPCRs. For pool-RT-qPCRs, date of sampling, time of registration and result communication, the name of the school, the name of the class, the number of students

per pool and the test result were transmitted. For single-RT-qPCRs, date of sampling, time of registration and result communication, the name of the school, the name of the class, age, gender and the test result were transmitted. From the digital database, data were transmitted to the University Hospital Cologne for retrospective analysis.

Retrospective analysis of the SARS-CoV-2 screening in daycare facilities

For retrospective analysis of the SARS-CoV-2 screening in daycare facilities, the University of Cologne was engaged by the Youth Welfare Office of the city of Cologne and approved by the IRB of the Faculty of Medicine, University Hospital of Cologne, Germany (number 21-1358). Since 15th of March 2021, voluntary SARS-CoV-2 testing was offered to all daycare facilities in Cologne within the SARS-CoV-2 screening program “Kita Testung Köln (KiKo)” under the direction of the Youth Welfare Office of the city of Cologne. Of all participating children and staff members, two Lolli-Swabs per week were tested in a pooled RT-qPCR. One diagnostic laboratory was involved in processing the Lolli-swabs. This laboratory transmitted anonymized, de-identifiable data to the University Hospital of Cologne for retrospective analysis weekly. Data were transmitted for pool-RT-qPCRs and single RT-qPCRs. For pool-RT-qPCRs, date of sampling, time of registration and result communication, the name of the daycare facility, the name of the group, the number of individuals per pool and the test result were transmitted. For single-RT-qPCRs, date of sampling, time of registration and result communication, the name of the daycare facility, the name of the group, age, gender and the test result were transmitted.

Instructions for the SARS-CoV-2 screenings in schools and daycare facilities

All staff, parents and children were instructed by either the Ministry of Education and Schools of North Rhine-Westphalia or the Youth Welfare Office of the city of Cologne. Written instructions in 12 different languages as well as instructional videos were used for training of all involved individuals. In addition, information and instructions for parents, children and staff were made available online (https://www.schulministerium.nrw/lolli-tests, https://www.kita-testung-koeln.de)

Sample processing

Validation of the Lolli-Method

To determine the sensitivity of the Lolli-Method, matched Lolli-swabs and Np/Op-swabs of acutely infected individuals were obtained. The participants were instructed to suck on a regular swab it for 30 seconds. Very young children were supported by either their parents or a physician. Afterwards, a physician took an Np-/Op-swab.

To find out, whether the time of day at which the samples were taken had an impact on the sensitivity, the individuals were sampled either in the morning, one hour after breakfast or at any time of the day. The impact of the pooling process on the measured viral loads was determined by obtaining two Lolli-swabs from the same participant at the same time. One sample was tested in a pool-RT-qPCR with up to 17, 49 or 99 negative samples and the corresponding sample was tested in a single-RT-qPCR. To determine whether the detection rate depends on a particular swab type that is used for the sampling, the following four types of swabs were used for sample collection of Lolli-swabs: A) Oropharyngeal swab, Copan, catalog number: 801U059, B) Nasopharyngeal swab, Biocomma, catalog number: YVJ-TE4, C) Oropharyngeal swab, Biocomma, catalog number: YVJ-TE4, D) Dry swab, Sarstedt, catalog number: 1U059S01.

When tested in a single-RT-qPCR, each Lolli-swab was placed in a 2 ml tube pre-filled with 2 ml phosphate buffered saline (PBS), moved up and down and pressed against the bottom of the tube repetitively for 20 seconds. The Np/Op-swabs were vortexed in the viral transport media for 20 seconds. When tested in a pool-RT-qPCR, a Lolli-swab of one acutely infected individual was tested in a pool with 17, 49 or 99 Lolli-swabs of individuals not infected with SARS-CoV-2. A pool of Lolli-swabs was processed by placing the Lolli-swabs in one 50 ml centrifugation tube, adding 3 ml PBS and vortexing for 30 seconds. Of all samples, 1 ml each was used for SARS-CoV-2 detection.

SARS-CoV-2 screening in schools and daycare facilities

Lolli-swabs were used as described above for the sampling of the students in schools and children and the staff in daycare facilities. The staff was instructed for self-sampling and supervising of the sampling of the children. The samples of all participants of the same daycare group or school class were placed in one 50 ml centrifugation tube and transported to one of the 12 diagnostic laboratories. 3 ml PBS were pipetted in one centrifugation tube. The tube was vortexed for 30 seconds.

SARS-CoV-2 detection and quantification

Validation of the Lolli-Method

For SARS-CoV-2 detection, either COBAS 6800 (Roche Diagnostics) and Alinity m (Abbott) instruments equipped with their respective SARS-CoV-2 detection kits, or the Quantstudio 5 (Thermofisher) instrument, using the Quick-RNA Viral Kits (Zymo Research) for RNA isolation and GeneFinder™ COVID-19 Plus RealAmp was used.

For the comparison of cycle threshold (Ct) values measured by the different RT-qPCR equipments, Ct-values were translated into copies/ml. To this end, seven serial

dilutions from a high titer SARS-CoV-2 sample were tested in all RT-qPCR equipments described above. With help of a regression model, standard curves for each equipment were generated. For the following conversion of device-specific Ct-values into copies/ml, two SARS-CoV-2 samples with a quantified RNA load from INSTAND (Society for the Promotion of Quality Assurance in Medical Laboratories, e.V., Düsseldorf, Germany; in cooperation with the Robert Koch-Institute and the Institute of Virology, Charité, Berlin) were tested on every device and subsequently used for Ct-based absolute RNA quantification.

SARS-CoV-2 screening in schools and daycare facilities

For SARS-CoV-2 detection, the 12 laboratories reported to use different equipment which is listed in Supplementary Table 3. Viral load was reported as Ct-value.

Adapting the SEIR-Model for a SARS-CoV-2 screening of children

A compartmental epidemiological model was used to study the efficiency of a long-term SARS-CoV-2 screening based on the Lolli-Method. The model consists of a closed population of N individuals and four possible states for each of them: Susceptible (S), Exposed (E), Infected (I) and recovered (R) (Figure 1i). Those states were chosen based on the impact that a long exposed period has on the epidemiological dynamics and on testing-based non-pharmaceutical interventions[39].

Susceptible individuals get infected by a transmission within the population (internal infection rate) or by an exogenous transmission from outside the population (external infection rate), at rates r_1 and r_2 respectively. Overall, the total infection rate of susceptible individuals is given by

(1)

$$r = ar_1 + (1 - a)r_2$$

where a is the fraction of time that individuals interact within the test- population.

(2)

$$a = \frac{5\,\frac{hours}{day} \times 5\ weekdays}{12\,\frac{hours}{day} \times 7\ day} \approx 0.3$$

was chosen in order to approximate interactions within the test-population only occurring 5 hours per day during weekdays (Mon-Fri) and assuming that on average there are in total 12 hours per day of interaction in and outside the test-population. The internal infection rate is defined as

(3)

$$r_1 = \frac{\beta I}{N}$$

and the external infection rate as

(4)

$$r_2 = \beta\pi$$

where I is the total number of infectious individuals in the population, π is the global prevalence and β is the infection-causing contact rate between individuals.

An infected individual that is in the exposed state moves into the infectious state at a constant rate of r_e:

(5)

$$r_e = \frac{1}{\tau_e}$$

From the infectious state, an infected individual moves to the recovered state at a constant rate of r_i:

(6)

$$r_i = \frac{1}{\tau_i}$$

These two last stochastic transitions follow homogeneous Poisson processes and therefore, exposed and infectious periods in the population follow exponential distributions with corresponding means τ_e and τ_i.

Implementing the sensitivity of the Lolli-Method in the extended SEIR-model

The probability of a positive test result when testing an exposed or infected individual is p_{det} given by

(7)

$$p_{det} = p_{PCR} \times S(VL)$$

where $1 - p_{PCR}$ is the false-negative rate of RT-qPCR and $S(VL)$ is a viral load dependent sensitivity function. To estimate $S(VL)$, we fit the measured sensitivity data to a sigmoidal function

(8)

$$S(VL) = \frac{1}{1 + \left(\frac{log_{10}VL}{log_{10}VL_{50}}\right)^{-\delta}} \pm 1.96\sigma_S,$$

where VL_{50} and δ are fit parameters. VL_{50} corresponds to the viral load at which $S(VL_{50}) = 0.5$ and δ quantifies the steepness of the sigmoidal function. We used the function *curve_fit* from the *scipy.optimize* library that implements a least squares

method. The standard deviation for the fitted curve σ_S was calculated with standard error propagation from the standard deviations of the fitted parameters, $\sigma_{VL_{50}}$ and σ_δ, as

(9)

$$\sigma_S = \frac{\left(\frac{log_{10}VL}{log_{10}VL_{50}}\right)^{-b}}{\left(\left(\frac{log_{10}VL}{log_{10}VL_{50}}\right)^{-b} + 1\right)^2} \sqrt{\left(\frac{\delta}{log_{10}VL_{50}}\right)^2 \sigma_{VL_{50}}^2 + \left(\log\frac{log_{10}VL}{log_{10}VL_{50}}\right)^2 \sigma_\delta^2},$$

such that $\pm 1.96\sigma_S$ represents 95% confidence level.

In order to determine the time dependence of the sensitivity of the Lolli-Method (days since infection), it was assumed that infected individuals would have a viral load of 10^6 copies/ml three days after infection. We assume exponential growth for the viral load with constant rate g:

(10)

$$VL(t) = e^{gt}$$

Temporal dynamics of viral load and the associated sensitivity of the Lolli-Method are relevant because it was assumed that on average infectiousness would begin three days after infection (Fig. 1j). Thus, in this model, transmissions within the institutions can only take place when the infection occurred at least three days ago. Infected individuals would be infectious on average for 6 days. A summary of model inputs can be found in Supplementary Table 1[37,40–48].

The numerical dynamics consist of continuous-time and individual-based simulations, in which the transitions between states of each individual are stochastically determined using the Gillespie algorithm. Additionally, a testing scheme was implemented in which infected individuals were tested positive according to

$p_{det}(t)$. Detected individuals were removed from the interacting population and the rest of the population was quarantined for the next 14 days one day after the detection. After this period, individuals could interact again. In this way, infected individuals that were not tested positive could transit to a recovered state without infecting other individuals in the test-population. We simulated testing protocols of 1 test per week (on Wednesday), 2 tests per week (Tuesday and Thursday) and 3 days per week (Monday, Wednesday and Friday.)

Calculation of 7-day pool incidence in schools

Pool-sizes were estimated by a linear model using official data by the Ministry of Schools and Education of North Rhine-Westphalia on class sizes and available reported pool-sizes (Supplementary Fig. 10a). During the first three weeks of the screening, students were taught and tested in a split-class lesson model, while a full-class lesson model was the basis of lessons and testing for the rest of the screening. During split-class lessons, 50% of the students of one class attended lessons and were tested on Mondays and Wednesdays. The other 50% of the students attended lessons and were tested on Tuesdays and Thursdays. During full-class lessons, the whole class attended lessons daily and was tested either Mondays and Wednesdays or Tuesdays and Thursdays (Supplementary Fig. 10b). Pool sizes were reported by the tested schools (Supplementary Fig. 10c). Means of class-sizes per school and means of reported pool-sizes per school were mapped as part of a linear model with a forced Y-axis intercept of 0. (Supplementary Fig. 10d) Slopes during spit-class lessons were m=0.97 and during full-class lessons m=0.97 before and 0.96 after summer holidays. Thus, reported average pool-sizes per school corresponded to approximately 97% and 96%, respectively, of the average class-sizes per school. For this reason, average class-sizes per school were used as an estimate of the average pool-sizes per school

for the estimation of number of children tested and the subsequently calculated 7-days-pool-incidence (pool-incidence= number of positive pool-RT-qPCRs/100.000 tested children in 7 days)

School social deprivation index (SSDI)

The level of social deprivation of schools is measured by a nine-level school social deprivation index (SSDI). The index is generated via a confirmatory factor analysis with four indicator variables[22]. The latent variable is divided into nine classes: Level 1 corresponds to a very low social deprivation; level 9 corresponds to a very high social deprivation. The index is based on several school-related indicators:

1. Child and youth poverty in the vicinity of an elementary school
2. Proportion of students with predominantly non-German family languages
3. Proportion of students who have moved to Germany from abroad
4. Proportion of students with special educational needs for learning, emotional and social development and language

The selection of the indicators is based on two criteria: First, to reflect socio-demographic variables relevant to school performance, and second, to avoid additional data collection and to use data that are uniformly available across the state.

With the exception of the indicator for child and youth poverty, all data come from the official school statistics of the state of North Rhine-Westphalia. A kernel-density estimate for the residential addresses of minors in unemployment/social-assistance-beneficiary households from the statistics of the Federal Employment Agency forms the indicator for child and youth poverty. It is a location statistic that shows the spatial density of minors in the vicinity of schools. The fourth indicator is included in the model as an interaction indicator (indicator of child and youth poverty * proportion of students with special educational needs). Therefore, a correlation between the interaction

indicator and the indicator for children and youth poverty was allowed in the factor model.

The index shows good explanatory power for different learning outcomes when evaluated with the results of the centrally organized performance assessments VERA 3 (e.g. correlation with reading comprehension in German results in R^2 = 0.39).

The SSDI was formed for each school as a superordinate unit of several locations. These locations are referred to in the manuscript as „schools". The analysis of the correlation between SSDI and SARS-CoV-2 infections is based on the test data from these locations, but is carried out using the school as the superordinate unit.

SARS-CoV-2 infection dynamics in schools

Estimating the differences between SARS-CoV-2 variants in infection dynamics in schools was based on the notion that transmissions inside school classes (in-class transmissions) should lead to an excessive number of pool-RT-qPCRs containing more than one infected child. We implemented this notion by first estimating the expected number of pool-RT-qPCRs with more than one infected child assuming a Null model without in-class transmissions. We next compared the expected number of pool-RT-qPCRs with more than one infected child to the observed number of pool-RT-qPCRs with more than one infected child.

Positive pool-RT-qPCRs were filtered based on the following criteria to ensure only high-quality data is used for this analysis: i) only pool-RT-qPCRs that have a matching positive single-RT-qPCR, ii) number of following single-RT-qPCRs is within 20% of the pool size.

First, we calculated the probability of each tested child being infected under the Null model. To calculate the probability of each tested child being infected, we fitted a single logistic regression model for the entire testing period (calendar week 19-25, 34-

37) using the local (district level) 7-day incidence of children aged between 6 and 10 years, the rate of positivity of pool-RT-qPCRs per district and per calendar week and the school social deprivation index (SSDI) as predictors (covariates),

(11)

$$p(P_{iw}) = p_{iw} = \beta_1 \cdot I_{iw} + \beta_2 \cdot PR_{iw} + \beta_3 \cdot SSDI_i + \beta_4 \cdot I_{iw}SSDI_i + \beta_5 \cdot PR_{iw}SSDI_i$$

where P_{iw} is the event that a specific child in a positive pool-RT-qPCR in school *i* and week *w* is tested positive, p_{iw} is the probability of being infected per child, $I_{iw}$is the local 7-day incidence among children aged between 6 and 10 years, PR_{iw} is the rate of positivity of pool-RT-qPCRs per district and per calendar week *w*, $SSDI_i$ is the school social deprivation index of school *i* and β_{1-5} are the regression coefficients.

After fitting the above regression coefficients, we calculated the probability of being infected per child p_{iw} for each positive pool RT-qPCR. Each such pool contains at least one infected child by definition. We computed the probability of observing additional infected children assuming a binomial distribution,

(12)

$$P(X) = \frac{n}{k} \cdot {p_{iw}}^k \cdot (1 - p_{iw})^{n-k}$$

where p_{iw} is the probability of each child being infected derived from the logistic regression model above, *n* is the number of tested children in a pool-RT-qPCR and *k* is the number of additional infected children. Using this binomial distribution, we computed the expected number of pool-RT-qPCRs with more than one infected child under the Null model (i.e. assuming no in-class transmissions). These values were compared to the observed number of pool-RT-qPCRs with more than one infected child in a given time period.

Statistical analysis

Geometric means were calculated for viral loads. Differences in viral loads were calculated with Wilcoxon-signed rank test (WSR) and Friedman test (FT). P-values <0.05 were considered significant. Sensitivity (positive percent agreement) and specificity (negative percent agreement) were calculated using RT-qPCR agreement. Differences in Ct-values during the screening program were calculated with Mann-Whitney test (MWT). Data analyses were done using the software GraphPad Prism (v.9), Microsoft Excel for Mac (v.14.7.3.) and R programing language (v. 3.5.2, stats package).

Additional Software

Maps of North Rhine-Westphalia and Cologne were designed with the iMapU tool provided by iExcelU.

Data availability

The data that support the findings of this study are provided with this paper. Source data are provided in Supplementary Data 1-6 and Supplementary Table 2.

Code availability

Codes of the epidemiological simulations are available in the Github repository https://github.com/betoto008/lolli_testing[49] and in Supplementary Data 7. Codes of the statistical modelling are available in the Github repository https://github.com/beyergroup/Lolli-Test-NRW.git[50] and in Supplementary Data 8.

References

1. Christophers, B. *et al.* Trends in clinical presentation of children with COVID-19: a systematic review of individual participant data. *Pediatr. Res.* **10**, 1390-020-01161–3 (2020).
2. Tagarro, A. *et al.* Screening and Severity of Coronavirus Disease 2019 (COVID-19) in Children in Madrid, Spain. *JAMA Pediatr.* e201346 (2020).
3. Ward, H. *et al.* SARS-CoV-2 antibody prevalence in England following the first peak of the pandemic. *Nat. Commun.* **4**, 100098 (2021).
4. Say, D. *et al.* Post-acute COVID-19 outcomes in children with mild and asymptomatic disease. *Lancet Child Adolesc. Heal.* **5**, e22–e23 (2021).
5. Jones, T. C. *et al.* Estimating infectiousness throughout SARS-CoV-2 infection course. *Science (80-.).* **973**, eabi5273 (2021).
6. Chu, V. T. *et al.* Household Transmission of SARS-CoV-2 from Children and Adolescents. *N. Engl. J. Med.* **385**, 954–956 (2021).
7. Covid 19 and School Closures: One Year of Education Disruption. *Unicef* (2021).
8. Hawrilenko, M., Kroshus, E., Tandon, P. & Christakis, D. The Association between School Closures and Child Mental Health during COVID-19. *JAMA Netw. Open* **4**, e2124092 (2021).
9. Lee, J. Mental health effects of school closures during COVID-19. *Lancet Child Adolesc. Heal.* **4**, 421 (2020).
10. Monnier, M. *et al.* Children’s mental and behavioral health, schooling, and socioeconomic characteristics during school closure in France due to COVID-19: the SAPRIS project. *Sci. Rep.* **11**, 1–15 (2021).
11. Pavelka, M. *et al.* The impact of population-wide rapid antigen testing on SARS-CoV-2 prevalence in Slovakia. *Science (80-.).* **372**, 635–641 (2021).

12. Im Kampe, E. O., Lehfeld, A. S., Buda, S., Buchholz, U. & Haas, W. Surveillance of COVID-19 school outbreaks, Germany, March to August 2020. *Eurosurveillance* **25**, 2001645 (2020).

13. Sherby, M. R. *et al.* SARS-CoV-2 screening testing in schools for children with intellectual and developmental disabilities. *J. Neurodev. Disord.* **13**, 31 (2021).

14. Young, B. C. *et al.* Daily testing for contacts of individuals with SARS-CoV-2 infection and attendance and SARS-CoV-2 transmission in English secondary schools and colleges: an open-label, cluster-randomised trial. *Lancet* **398**, 1217–1229 (2021).

15. Hoehl, S. *et al.* Longitudinal Testing for Respiratory and Gastrointestinal Shedding of Severe Acute Respiratory Syndrome Coronavirus 2 (SARS-CoV-2) in Day Care Centers in Hesse, Germany. *Clin. Infect. Dis.* **73**, e3036–e3041 (2021).

16. Willeit, P. *et al.* Prevalence of RT-qPCR-detected SARS-CoV-2 infection at schools: First results from the Austrian School-SARS-CoV-2 prospective cohort study. *Lancet Reg. Heal. - Eur.* **5**, 100086 (2021).

17. Corman, V. M. *et al.* Comparison of seven commercial SARS-CoV-2 rapid point-of-care antigen tests: a single-centre laboratory evaluation study. *The Lancet Microbe* **2**, e311–e319 (2021).

18. Aiano, F. *et al.* Feasibility and acceptability of SARS-CoV-2 testing and surveillance in primary school children in England: Prospective, crosssectional study. *PLoS One* **16**, e0255517 (2021).

19. Vandenberg, O., Martiny, D., Rochas, O., van Belkum, A. & Kozlakidis, Z. Considerations for diagnostic COVID-19 tests. *Nat. Rev. Microbiol.* **Epub ahead**, 1–13 (2021).

20. Walter, E. B. *et al.* Evaluation of the BNT162b2 Covid-19 Vaccine in Children 5

to 11 Years of Age. *N. Engl. J. Med.* **NEJMoa2116**, (2021).

21. Karim, S. S. A. & Karim, Q. A. Omicron SARS-CoV-2 variant: a new chapter in the COVID-19 pandemic. *Lancet (London, England)* **6736**, 19–21 (2021).

22. Schräpler, J. & Jeworutzki, S. *Konstruktion des Sozialindex für Schulen in Nordrhein-Westfalen*. (Zentrum für interdisziplinäre Regionalforschung (ZEFIR), Fakultät für Sozialwissenschaft, Ruhr-Universität Bochum, LOTA 38, 44780 Bochum, 2021).

23. Buonsenso, D. *et al.* Schools closures during the COVID-19 pandemic: A catastrophic global situation. *Pediatr. Infect. Dis. J.* e146–e150 (2021) doi:10.1097/INF.0000000000003052.

24. Ghosh, R., Dubey, M. J., Chatterjee, S. & Dubey, S. Impact of COVID-19 on children: Special focus on the psychosocial aspect. *Minerva Pediatr.* **72**, 226–235 (2020).

25. Woloshin, S., Patel, N. & Kesselheim, A. S. False Negative Tests for SARS-CoV-2 Infection — Challenges and Implications. *N. Engl. J. Med.* (2020) doi:10.1056/nejmp2015897.

26. Hoehl, S. *et al.* At-home self-testing of teachers with a SARS-CoV-2 rapid antigen test to reduce potential transmissions in schools Results of the SAFE School Hesse Study. *medRxiv* (2020) doi:10.1101/2020.12.04.20243410.

27. Allan-Blitz, L. T. & Klausner, J. D. A Real-World Comparison of SARS-CoV-2 Rapid Antigen Testing versus PCR Testing in Florida. *J. Clin. Microbiol.* **59**, e01107-21 (2021).

28. Joachim, A. *et al.* Pooled RT-qPCR testing for SARS-CoV-2 surveillance in schools- a cluster randomised trial. *EClinicalMedicine* **39**, 101082 (2021).

29. Willeit, P. *et al.* Prevalence of RT-PCR-detected SARS-CoV-2 infection at schools: First results from the Austrian School-SARS-CoV-2 Study. *medRxiv*

2021.01.05.20248952 (2021) doi:10.1101/2021.01.05.20248952.

30. Mendoza, R. P. *et al.* Implementation of a pooled surveillance testing program for asymptomatic SARS-CoV-2 infections in K-12 schools and universities. *EClinicalMedicine* **38**, 101028 (2021).

31. Goldfarb, D. M. *et al.* Self-collected saline gargle samples as an alternative to healthcare worker collected nasopharyngeal swabs for COVID-19 diagnosis in outpatients. *medRxiv* (2020) doi:10.1101/2020.09.13.20188334.

32. Wunsch, M. *et al.* Safe and Effective Pool Testing for SARS-CoV-2 Detection. *SSRN Electron. J.* (2020) doi:10.2139/ssrn.3684470.

33. Wunsch, M. *et al.* Safe and effective pool testing for SARS-CoV-2 detection. *J Clin Virol* **145**, 105018 (2020).

34. Li, Y. *et al.* The temporal association of introducing and lifting non-pharmaceutical interventions with the time-varying reproduction number (R) of SARS-CoV-2: a modelling study across 131 countries. *Lancet Infect. Dis.* (2020) doi:10.1016/S1473-3099(20)30785-4.

35. Lam-Hine, T. *et al.* Outbreak Associated with SARS-CoV-2 B.1.617.2 (Delta) Variant in an Elementary School — Marin County, California, May-June 2021. *MMWR Recomm. Reports* **70**, 1214–1219 (2021).

36. Van Loon, W. *et al.* Prevalence of SARS-CoV-2 Infections among Students, Teachers, and Household Members during Lockdown and Split Classes in Berlin, Germany. *JAMA Netw. Open* **4**, e2127168 (2021).

37. Campbell, F. *et al.* Increased transmissibility and global spread of SARS-CoV-2 variants of concern as at June 2021. *Eurosurveillance* **26**, 2100509 (2021).

38. Ismail, S. A., Saliba, V., Lopez Bernal, J., Ramsay, M. E. & Ladhani, S. N. SARS-CoV-2 infection and transmission in educational settings: a prospective, cross-sectional analysis of infection clusters and outbreaks in England. *Lancet*

Infect. Dis. **21**, 344–353 (2021).

39. Tovar, R. M., Gruell, H., Klein, F. & Lässig, M. Stochasticity of infectious outbreaks and consequences for optimal interventions. (2021).

40. Quilty, B. J. *et al.* Quarantine and testing strategies in contact tracing for SARS-CoV-2: a modelling study. *Lancet Public Heal.* **6**, e175–e183 (2021).

41. Walsh, K. A. *et al.* The duration of infectiousness of individuals infected with SARS-CoV-2. *J. Infect.* **81**, 847–856 (2020).

42. Centers for Disease Control and Prevention. COVID-19 Pandemic Planning Scenarios. *Centers Dis. Control Prev.* (2021).

43. Volz E, Mishra S, Chand M, Barrett JC, Johnson R, Geidelberg L, Hinsley WR, Laydon DJ, Dabrera G, O'Toole Á, Amato R, Ragonnet-Cronin M, Harrison I, Jackson B, Ariani CV, Boyd O, Loman NJ, McCrone JT, Gonçalves S, Jorgensen D, Myers R, Hill V, Jackson DK, F. N. Assessing transmissibility of SARS-CoV-2 lineage B.1.1.7 in England. *Nature* **593**, 266–269 (2021).

44. Davies, N. G. *et al.* Estimated transmissibility and impact of SARS-CoV-2 lineage B.1.1.7 in England. *Science (80-.).* **372**, eabg3055 (2021).

45. Alcoba-Florez, J. *et al.* Sensitivity of different RT-qPCR solutions for SARS-CoV-2 detection. *Int. J. Infect. Dis.* **99**, 190–192 (2020).

46. Kucirka, L. M., Lauer, S. A., Laeyendecker, O., Boon, D. & Lessler, J. Variation in False-Negative Rate of Reverse Transcriptase Polymerase Chain Reaction-Based SARS-CoV-2 Tests by Time Since Exposure. *Ann. Intern. Med.* **173**, 262–267 (2020).

47. Vogels, C. B. F. *et al.* Analytical sensitivity and efficiency comparisons of SARS-CoV-2 RT–qPCR primer–probe sets. *Nat. Microbiol.* **5**, 1299–1305 (2020).

48. Goyal, A., Reeves, D. B., Fabian Cardozo-Ojeda, E., Schiffer, J. T. & Mayer, B.

T. Viral load and contact heterogeneity predict sars-cov-2 transmission and super-spreading events. *Elife* **10**, e63537 (2021).

49. Tovar, R. M. Effective high-throughput RT-qPCR screening for SARS-CoV-2 infections in children, betoto008/lolli_testing: Lolli testing. (2022) doi:10.5281/ZENODO.6491118.

50. Johnen, R. Effective high-throughput RT-qPCR screening for SARS-CoV-2 infections in children, beyergroup/Lolli-Test-NRW. (2022) doi:10.5281/ZENODO.6497682.

Acknowledgements

We thank all participants of the validation of the Lolli-Method and all children and staff in tested daycare facilities and schools. We thank Sascha Nickel and Anne Fries as well all staff members of their daycare facilities for their impetus for the development of the Lolli-Method. We thank all members of the Institute of Virology, University Hospital Cologne. In particular, we thank Irina Fish, Ivonne Torre-Lage, Christina Hellriegel and Esther Milz for processing of SARS-CoV-2 samples and optimizing the logistics. We thank Carsten Tschirner (IExcelU) for supporting data vizualisation, Stephan Glaremin, Udo Neumann, Anja Kolb-Bastigkeit (Amt für Jugend, Arbeit und Soziales der Stadt Köln), Barbara Michaelis, Niklas Marizy (Gesundheitsamt Köln) for administrative support during implementation of the screening in Cologne. We thank Janna Seifried and Sindy Böttcher (Robert Koch Institute) for continuous support and discussions, Norbert Schmeißer and Frederik Schmeißer (Medeora GmbH Köln) for supporting data collection, Kim Zun-Gon, Florian Korte and Hendrik Schöneborn (Boston Consulting Group) for organizational support, Christoph Gusovius from the Ministry for Schools and Education of the State of North Rhine-Westphalia, and

Dietmar Klimas and Philip Graul (Labor ZotzKlimas, Düsseldorf, Germany) and Philipp Kirfel (Synlab) for supporting diagnostic analysis.

Author contributions

All authors contributed to sections relevant to their experience. F.D., F.K., R.K., I.S., G.F., A.B. and J.R. contributed to conception and design of the project. F.D. G.H.R., R.K., F.K., V.D.C., G.B.F., D.L.V., A.R.H., A.J., J.M.C., A.T.H., J.R.Q., K.S., M.M., J.C.L., C.H., L.T.W., E.H., E.K. and M.W. developed and validated the Lolli-Method. R.M.T. and M.L. developed the extension of the SEIR-model. G.Q., H.W., C.T., R.Z., H.J., A.P., I.H., P.C., F.J.S., P.P., G.K., C.K. performed RT-qPCRs during the screening programs. M.B., A.W., A.K., J.N. and A.L. partnered as public health scientists. F.D., R.J., J.G, G.S., F.B., J.K., A.K., C.G. and M.F. performed data analysis. M.H., R.J., J.P.S. and J.G. performed statistical analysis. F.D., L.J., and V.L. managed the administrative framework. F.K., G.F., A.B. and J.D. supervised the project. F.D., R.M.T., J.G., R.J. S.J. and J.P.S. wrote the draft manuscript. All authors were involved in editing of the final manuscript

Competing interest declaration

F.D., F.K. and R.K. hold EU-wide trademark protection for the terms “Lolli-Test” (018503959) and “Lolli-Methode” (018503958). All authors have no competing interests.

Additional Information

Supplementary Information is available for this paper.

Correspondence should be addressed to florian.klein@uk-koeln.de

Funding was provided by the German Ministry of Education and Research (BMBF) (registration number: 01KX2021) within Bundesweites Forschungsnetz „Angewandte Surveillance und Testung“ (B-FAST) project of the „NaFoUniMedCovid19“ consortium. Furthermore, funding was provided by the state of North Rhine-Westphalia and by the Bundesministerium für Bildung und Forschung (registration number: ZMI1-2521COR004).

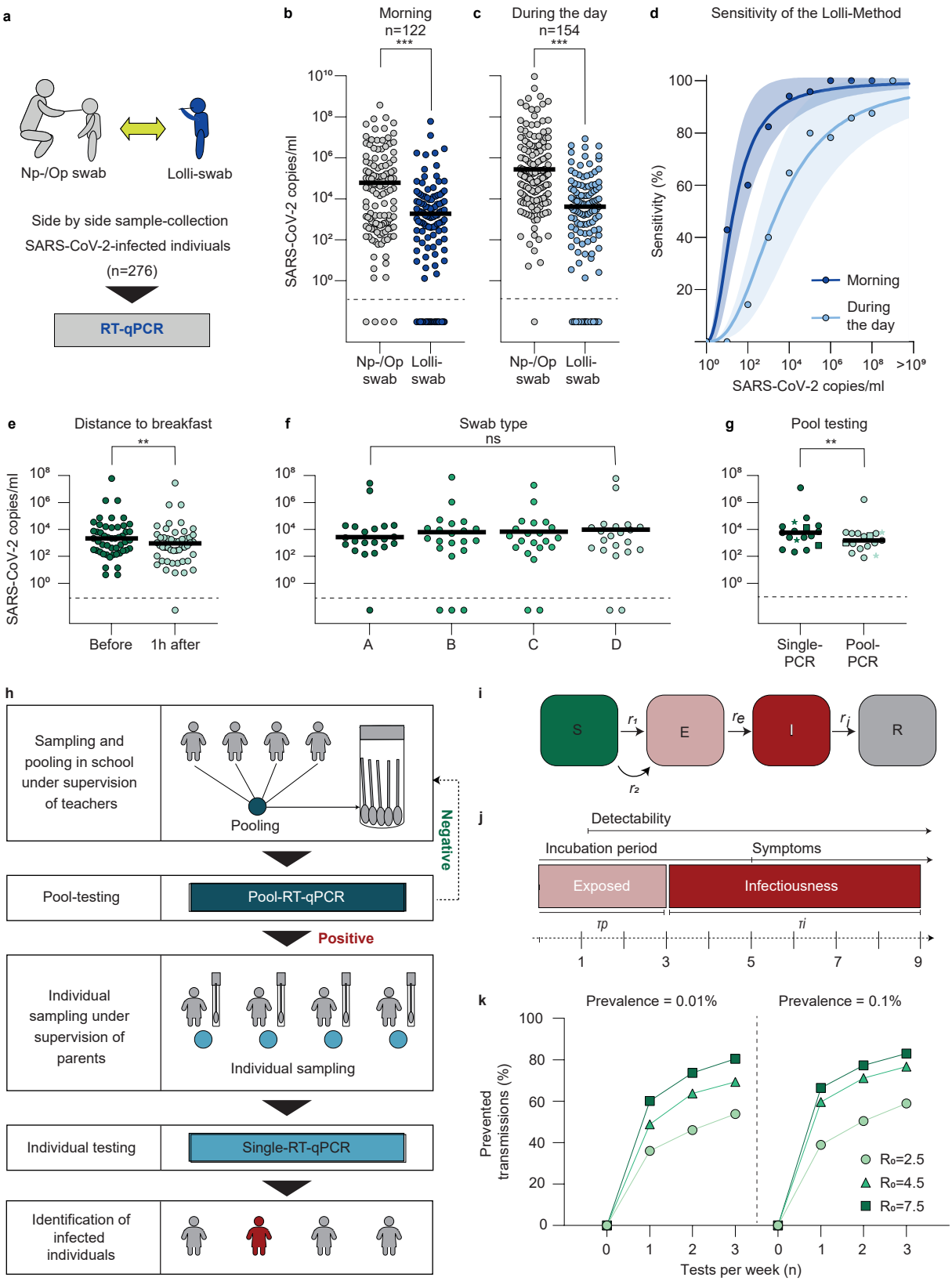

Fig. 1: Lolli-Method for high-throughput SARS-CoV-2 screening in children
a, Experimental design used to validate the Lolli-Method. **b**, Np-/Op-swabs and Lolli-swabs obtained in the morning plotted by viral load ($p<0.0001$, two-tailed Wilcoxon signed rank test, (WSR)). Horizontal lines represent mean viral loads. Asterisks represent p-values. **c**, Np-/Op-swabs and Lolli-swabs obtained during the day plotted by viral load ($p<0.0001$, two-tailed WSR). **d**, The sensitivity of the Lolli-Method is stratified by viral load as fit curve (least squares method), indicated by both blue lines. 95 % CI is indicated by colored area and time of sampling is indicated in corresponding colors. **e-g**, Matched Lolli-Swabs plotted by viral loads obtained in the morning and 1 hour after breakfast ($p=0.021$, two-tailed WSR) (e), with four types of Lolli-swabs ($p=0,72$, Friedmann test) (f), and for single-and pool-RT-qPCR, respectively ($p=0.017$, two-tailed WSR) (g). **g**, Dots represent pools of 18, squares of 49 and stars of 100 individuals. **h**, Visualization of the screening concept. Samples are pooled in the classroom and tested in RT-qPCR. Individual RT-qPCRs are tested the next day and only in case of a positive pool. **i**, SEIR-model to determine efficiency of the screening program. **j**, Assumptions for the course of a SARS-CoV-2 infection. **k**, Fractions of prevented transmissions stratified by test-frequency. Dots, triangles and squares represent SARS-CoV-2 basic reproduction values of 2.5, 4.5 and 7.5.

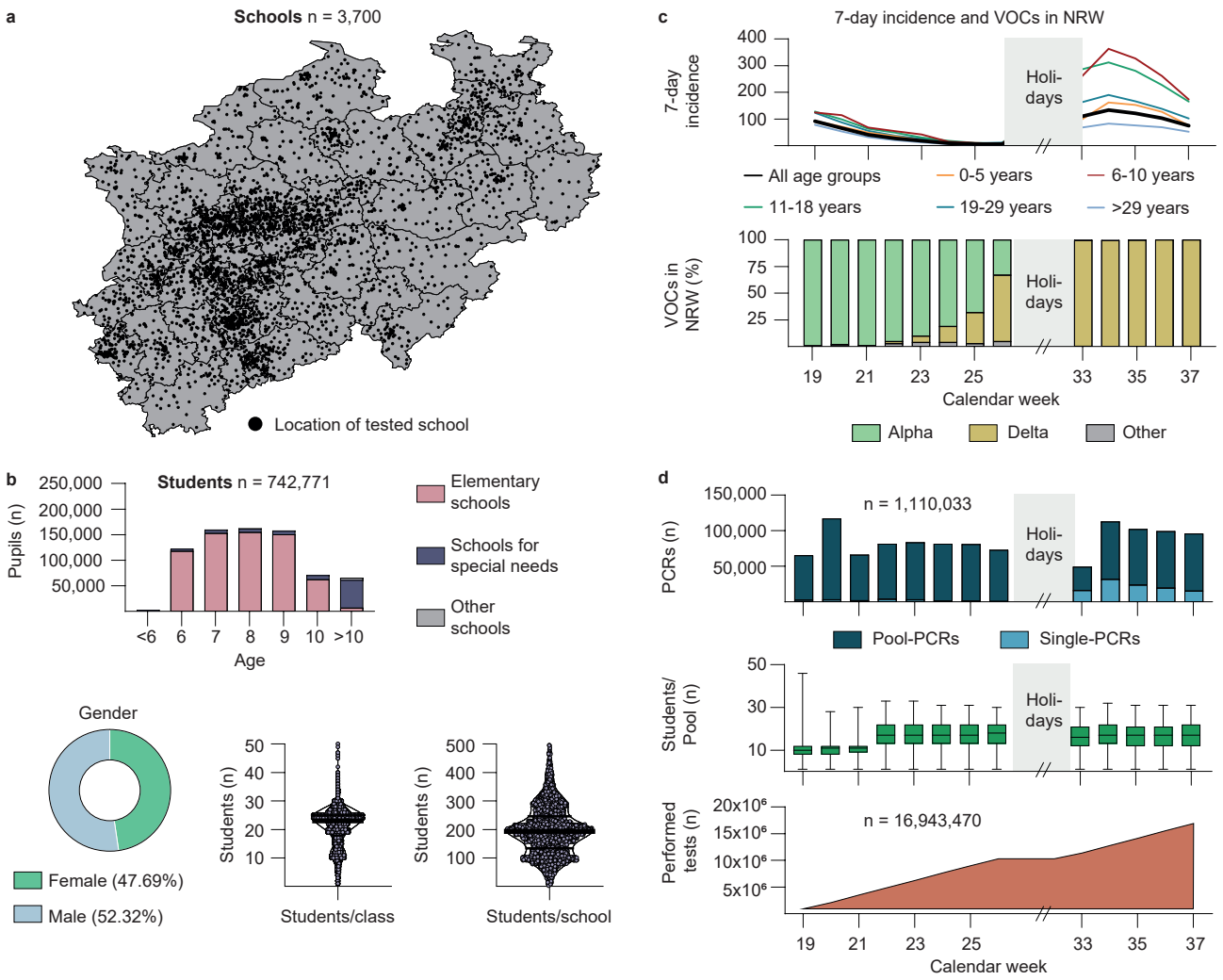

Fig. 2: Implementing the Lolli-Method screening concept in schools and daycare facilities
a, Map of North Rhine-Westphalia. Black dots mark the location of each school. **b**, Epidemiological characteristics of the tested students and characteristics of schools. Black horizontal lines in the violin plots represent median (M), first (Q1) and third (Q3) quartile (Students/class: M=23, Q1=18, Q3=25; Students/schools: M=193, Q1=134, Q3=246. **c**, 7-day incidence of different age groups (top) and frequency of variants of concern according to data published by the Robert Koch Institute (bottom) stratified by calendar week. Summer holidays are marked in grey. **d**, Number of performed RT-qPCRs (blue), average pool-sizes (green) and total number of performed tests are stratified by calendar week. The horizontal lines in the green Box-Whisker-Plot indicate the medians, the lines at the top and at the bottom of the boxes indicate first and third quartiles and the error bars represent minimum and maximum pool-sizes.

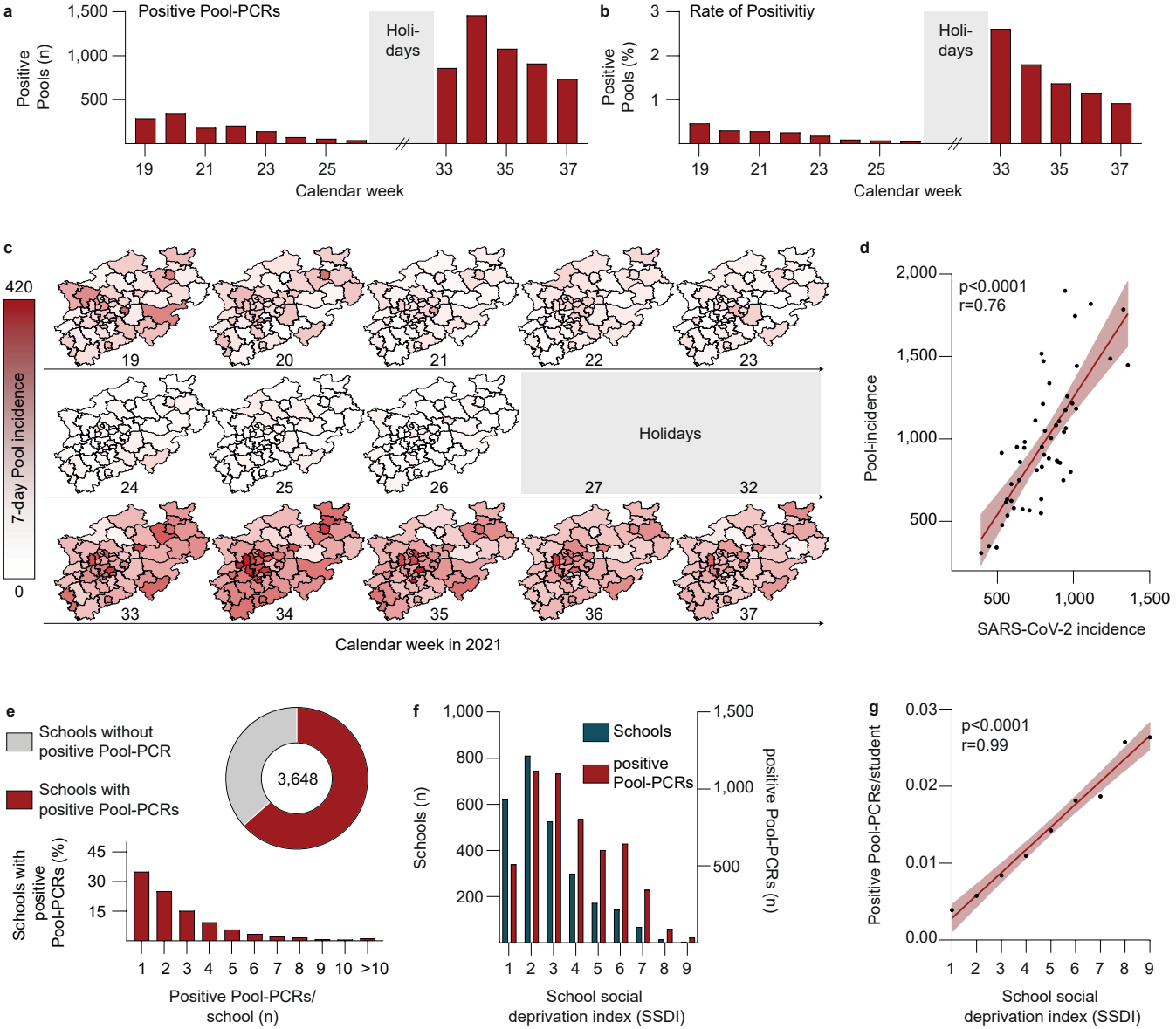

Fig. 3: Monitoring SARS-CoV-2 infections in schools
a, The number of positive pool-RT-qPCRs is stratified by calendar week. **b**, The rate of positivity of pool-RT-qPCRs stratified by calendar week. **c**, Maps of North Rhine-Westphalia depicting the 7-day pool-incidence per week and district. **d**, Spearman correlation (two-tailed) between pool-incidence and SARS-CoV-2 incidence ($p<0.0001$, $r=0.76$). Each black dot represents one district of North Rhine-Westphalia. 95% CI is indicated by the bright red area. **e**, Fraction of schools with at least one positive pool-RT-qPCR (pie-chart) and fraction of schools stratified by corresponding number of positive Pool-RT-qPCRs per school (bar chart). **f**, Number of schools and positive pool-RT-qPCR stratified by school social deprivation index level. **g**, Spearman correlation (two-tailed) between number of positive pool-RT-qPCRs/student and school social deprivation index level ($p<0.0001$, $r=0.99$). 95% CI is indicated by the bright red area.

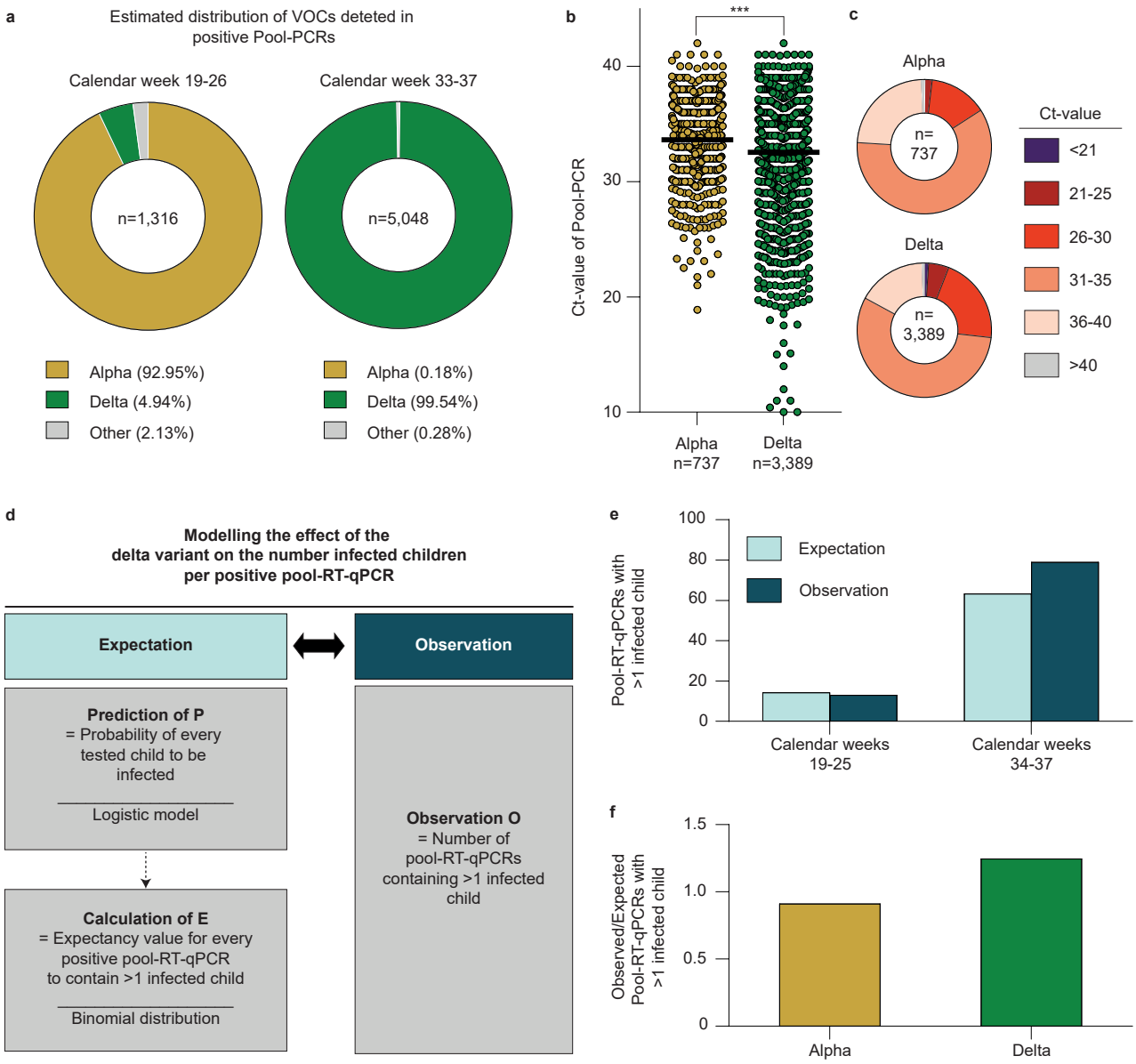

Fig. 4: High-throughput screening reveals differences in infection dynamics for SARS-CoV-2 variants in schools
a, Estimated distribution of VOCs during calendar weeks 19-26 and 33-37. VOCs are indicated by corresponding colors. **b**, All available Ct-values of positive pool-RT-qPCRs are plotted and stratified by estimated assignment to alpha (n=737 pools) or delta (n=3,389 pools) variant. Horizontal lines represent mean Ct-values, asterisks indicate the p-value ($p<0.0001$, two-tailed Mann-Whitney test). **c**, Categorization of Ct-values of positive Pool-RT-qPCRs assigned either alpha or delta variant in corresponding colors. **d**, Expected and observed numbers of positive pool-RT-qPCRs containing >1 infected child were compared by statistical modelling. **e**, The number of expected and observed positive pool-RT-qPCRs is stratified by time period. **f**, The ratio of expected and observed numbers of positive pool-RT-qPCRs containing >1 infected child is stratified by SARS-CoV-2 variant.

Supplementary Information
for
Effective high-throughput RT-qPCR screening for SARS-CoV-2 infections in children

Supplementary Figures

Supplementary Figure 1 Cohort of acutely infected individuals

Supplementary Figure 2 Pool-RT-qPCRs and testing areas of 12 laboratories

Supplementary Figure 3 Data collection and plausibility checks

Supplementary Figure 4 Turn-around time of RT-qPCRs

Supplementary Figure 5 Implementation of the Lolli-Method in daycare facilities

Supplementary Figure 6 Number of infected individuals in positive pool-RT-qPCRs

Supplementary Figure 7 Determination of the SARS-CoV-2 detection rate of the Lolli-Method

Supplementary Figure 8 Correlation between Ct-values of pool-RT-qPCR and matched single-RT-qPCRs

Supplementary Figure 9 Modelling differences in infections dynamics of SARS-CoV-2 variants with the Lolli-Method in schools

Supplementary Tables

Supplementary Table 1 SEIR-model parameter description

Supplementary Table 2 Tested schools and students

Supplementary Table 3 Equipment for SARS-CoV-2 screening in schools

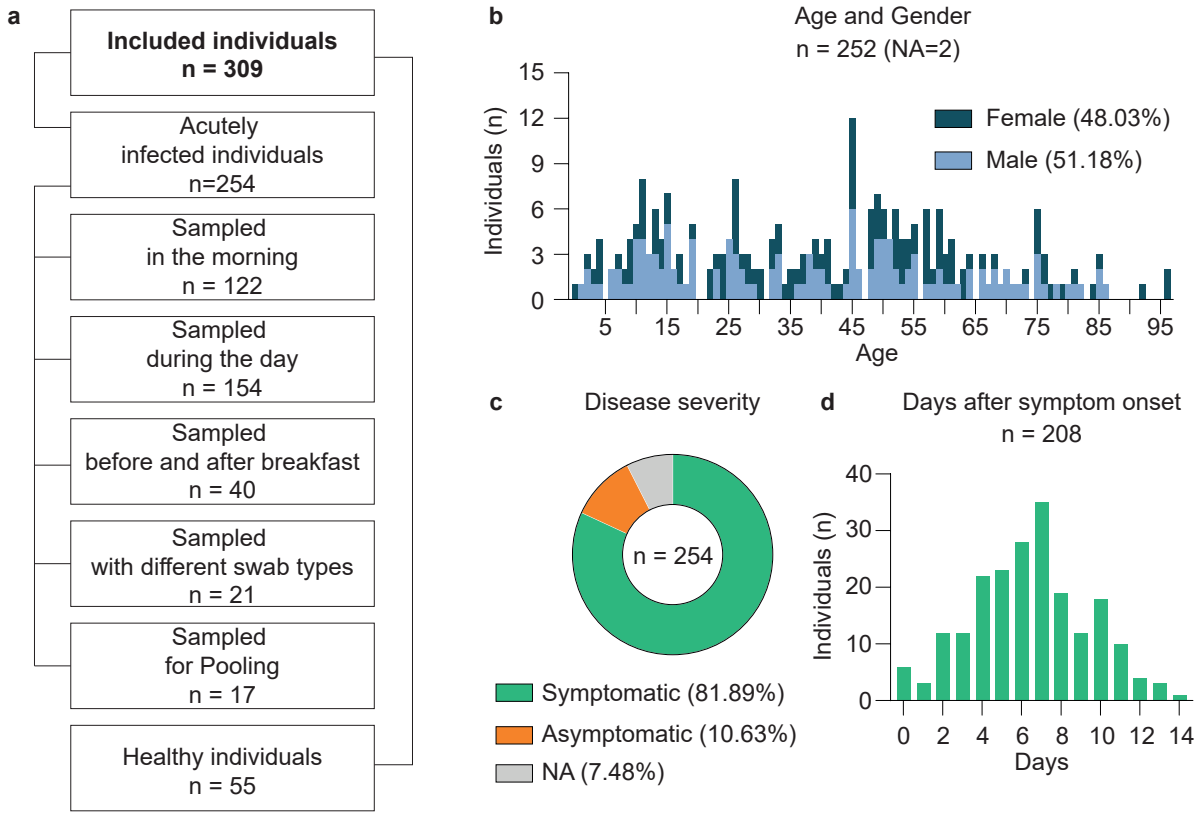

Supplementary Fig. 1: Cohort of acutely infected individuals
a, Flowchart including cohort sizes selected for RT-qPCR for the validation of the Lolli-Method. **b**, Age and gender distribution of the cohort. **c**, Disease severity among participants. **d**, Days after symptom onset among participants.

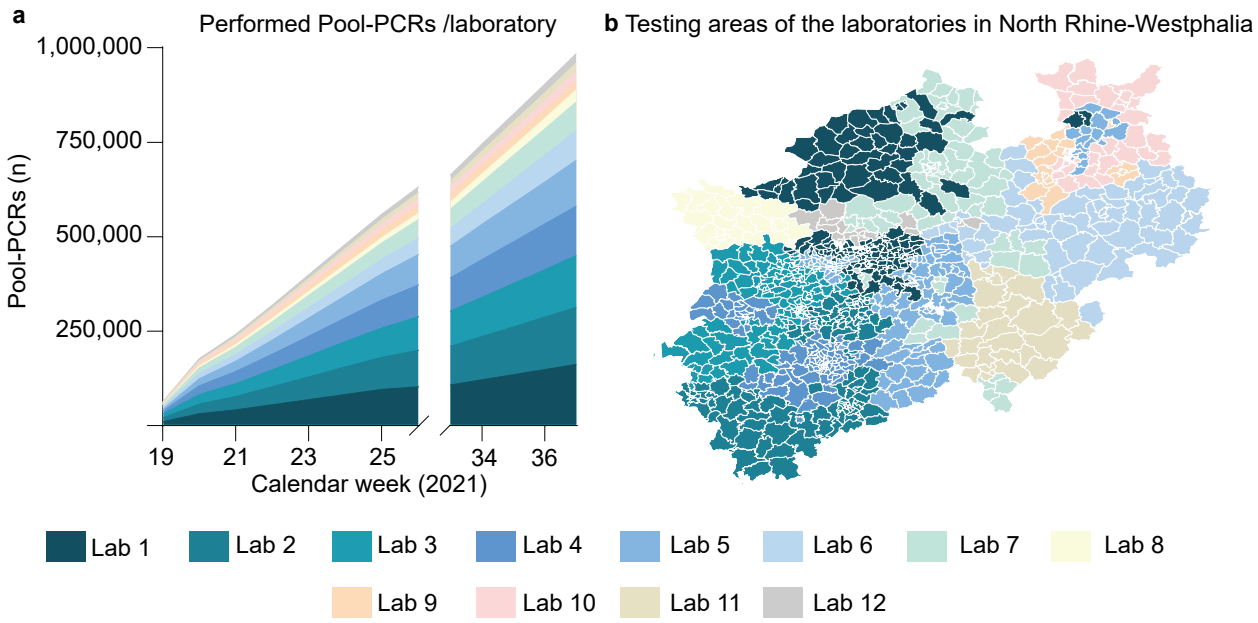

Supplementary Fig. 2: Pool-RT-qPCRs and testing areas of 12 laboratories
a, Cumulative number of performed pool-RT-qPCRs for each laboratory stratified by calendar week. **b**, Testing areas in North Rhine-Westphalia of each laboratory. Each laboratory is assigned one corresponding color.

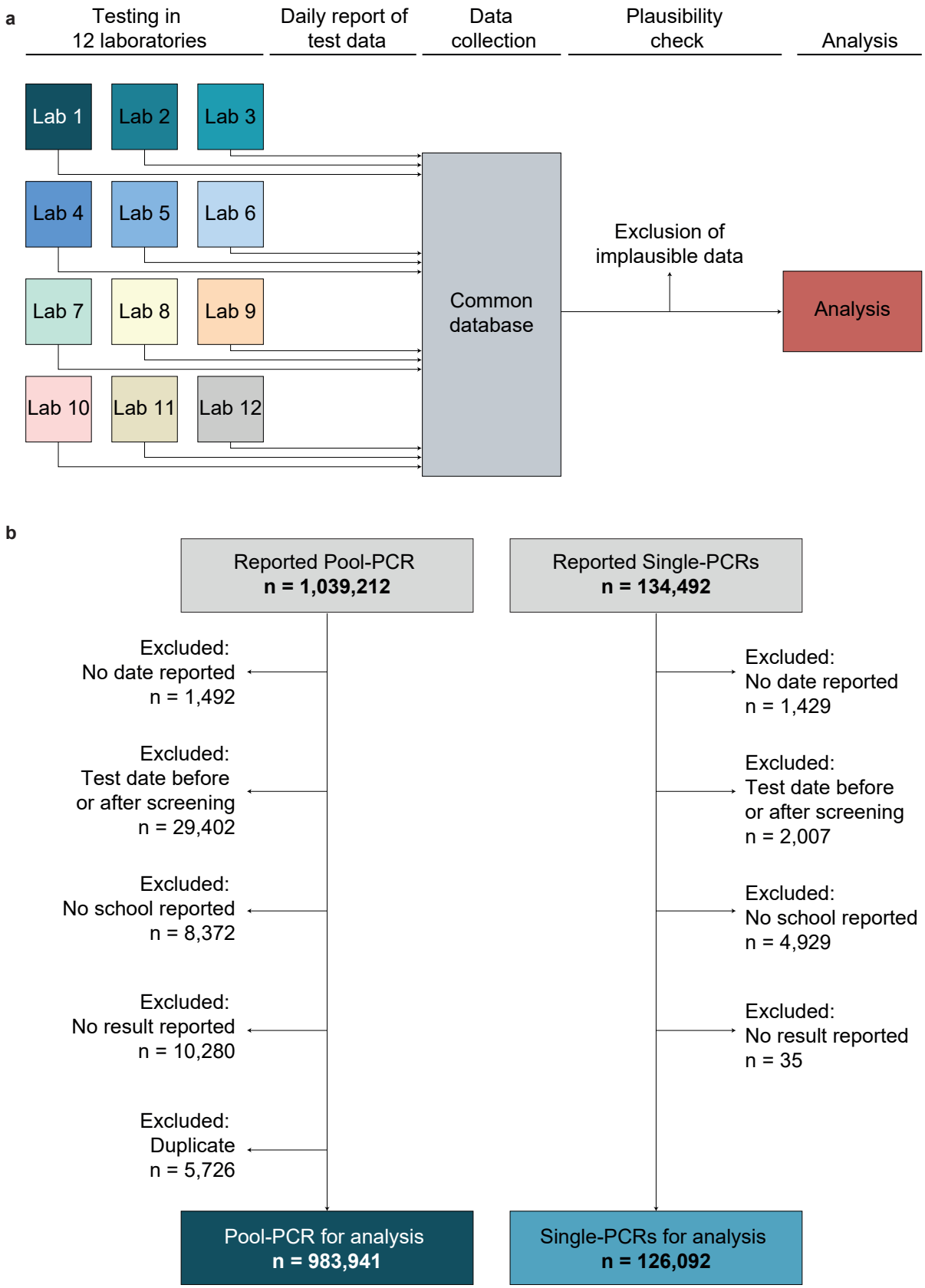

Supplementary Fig. 3: Data collection and plausibility checks
a, Flowchart including steps of data collection and quality control. **b**, Flowchart including details of data plausibility checks for RT-qPCRs indicating the numbers of RT-qPCRs that were used for analysis.

a Time of sample registration and result communication of Pool-PCRs

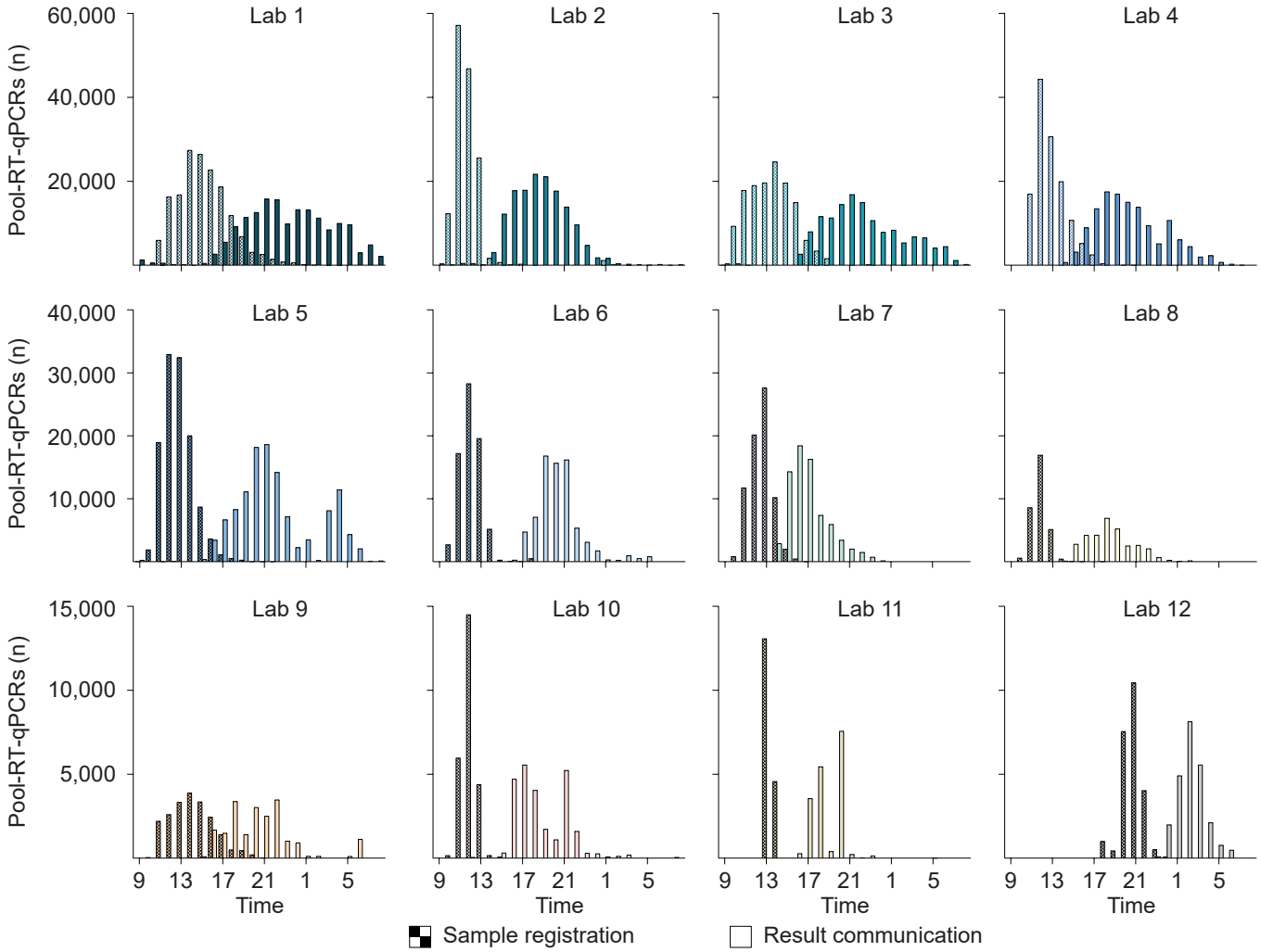

b Turn-around time of Pool-PCRs

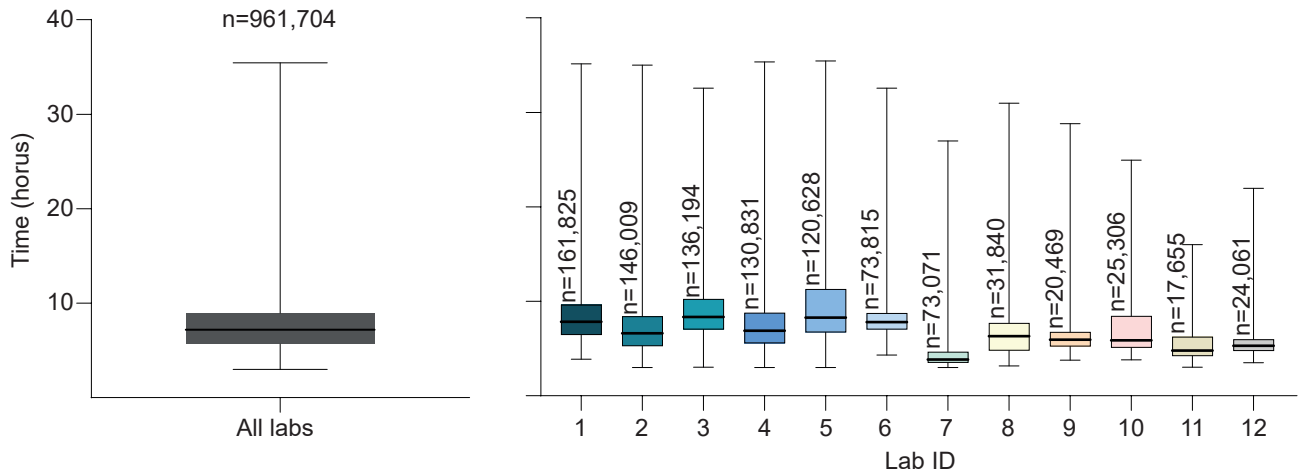

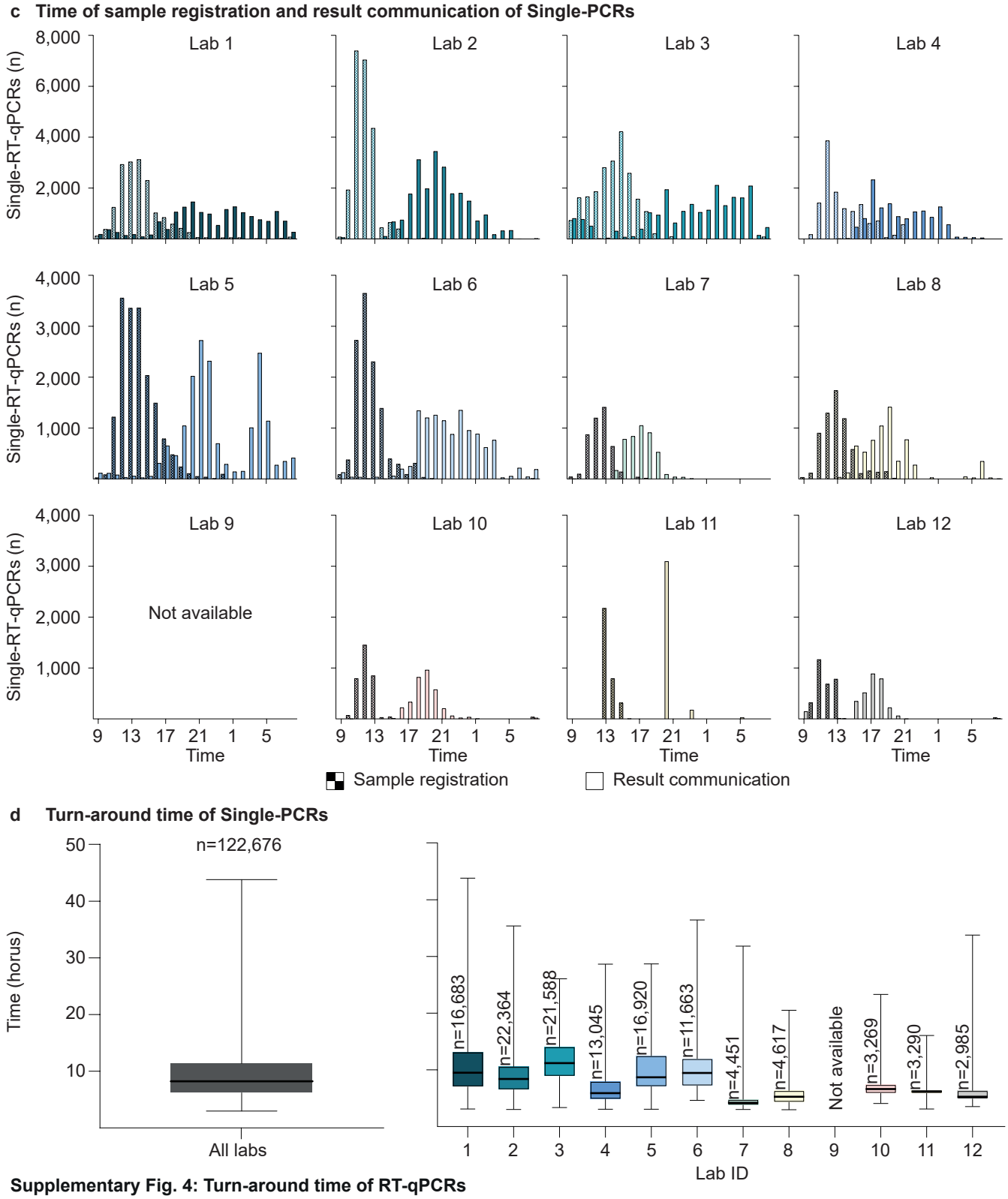

Supplementary Fig. 4: Turn-around time of RT-qPCRs

a, The bar charts represent the time of registration and result communication of pool-RT-qPCRs of each laboratory. **b**, Turn-around time of pool-RT-qPCRs (n=961,704 independent pool-RT-qPCRs). The horizontal lines in the green Box-Whisker-Plot indicate the medians, the lines at the top and at the bottom of the boxes indicate first and third quartiles and the error bars represent minimum and maximum turn-around times **c**, The bar charts represent the time of registration and result communication of single-RT-qPCRs of each laboratory. **d**, Turn-around time of single-RT-qPCRs (n=122,676 independent single-RT-qPCRs). The horizontal lines in the green Box-Whisker-Plot indicate the medians, the lines at the top and at the bottom of the boxes indicate first and third quartiles and the error bars represent minimum and maximum turn-around times.

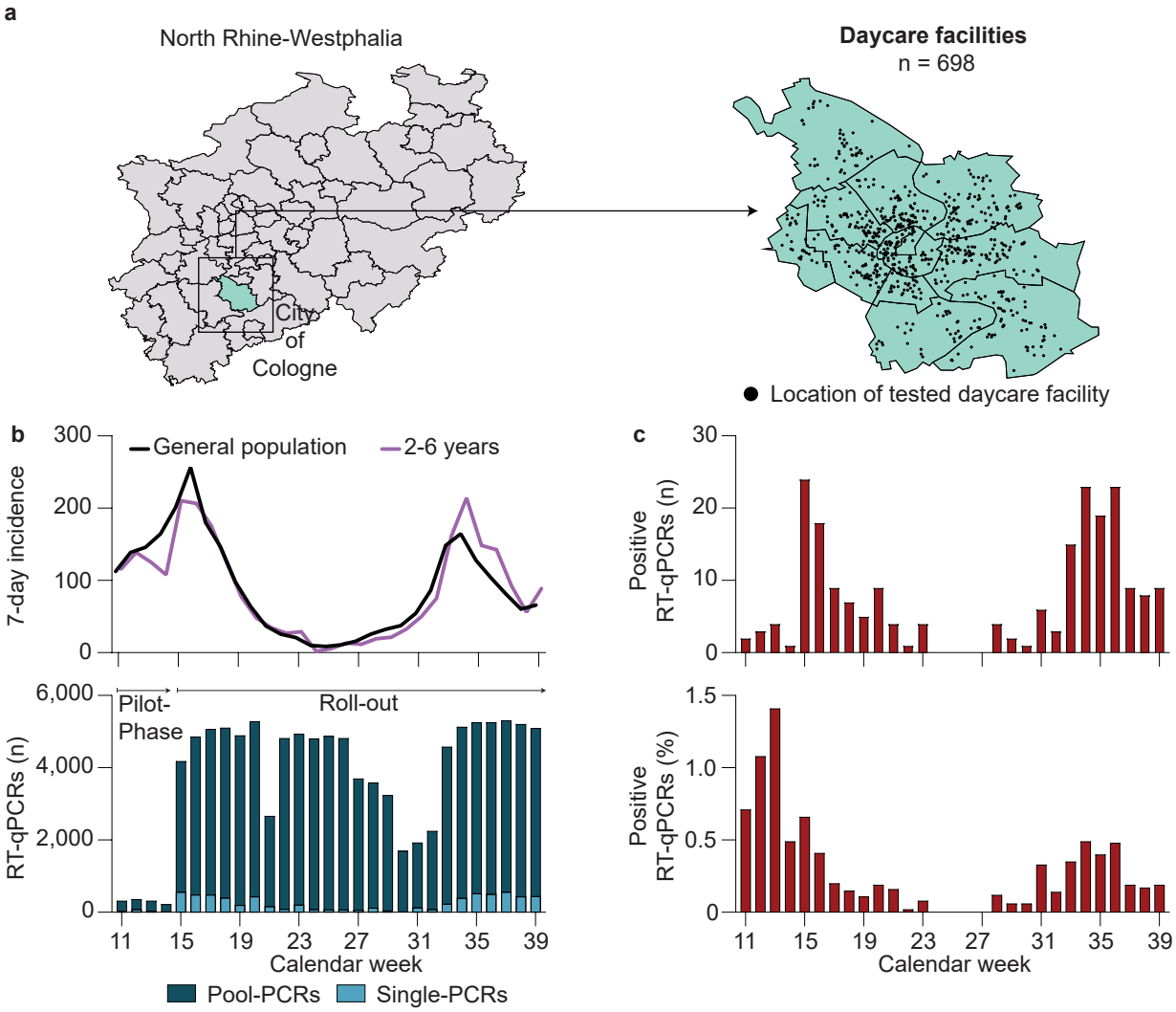

Supplementary Fig. 5: Implementation of the Lolli-Method in daycare facilities
a, Map of North Rhine-Westphalia indicating the locations of the tested daycare facilities in the city Cologne. **b**, SARS-CoV-2 7-day incidence in Cologne (top) and number of performed RT-qPCRs (bottom) stratified by calendar week. **c**, Number of positive pool-RT-qPCRs and rate of positivity of pool-RT-qPCRs stratified by calendar week.

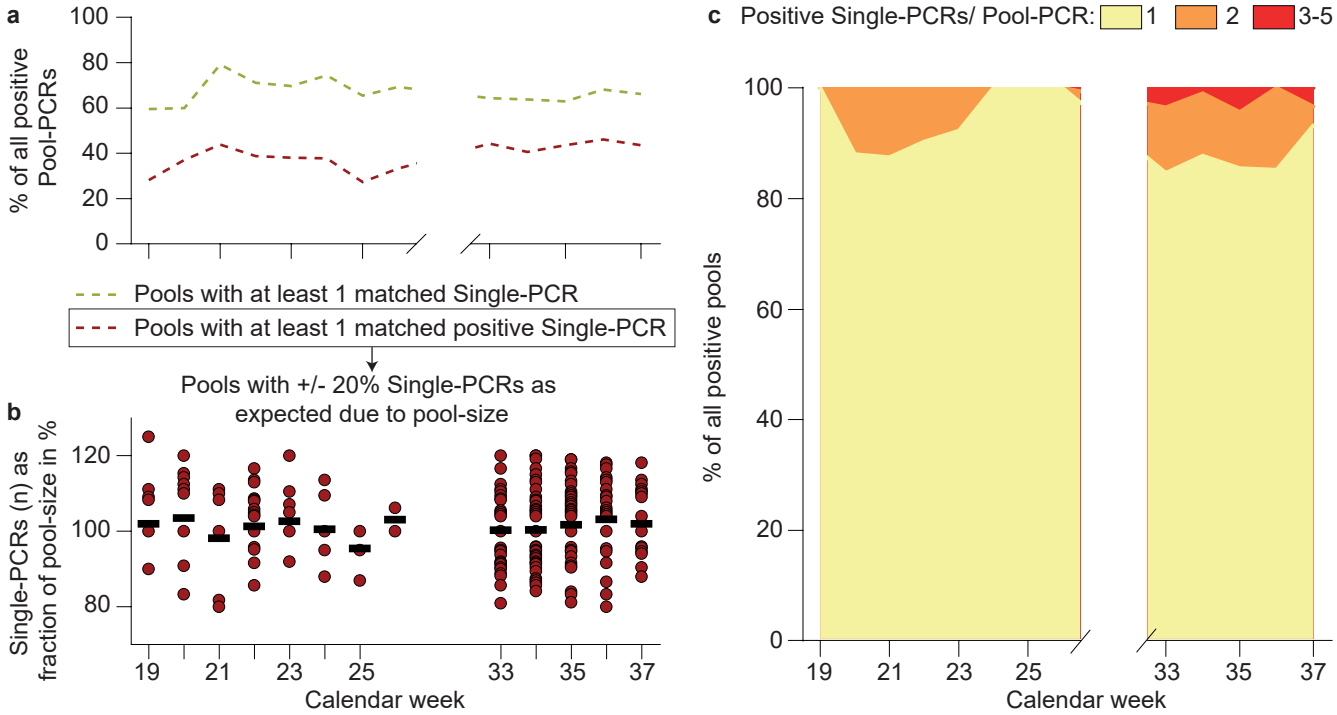

Supplementary Fig. 6: Number of infected individuals in positive pool-RT-qPCRs
a, Overview on data quality stratified by calendar week. **b**, Only pool-RT-qPCRs with at least one assigned positive single-RT-qPCR were used for further analysis. Out of those, only pool-RT-qPCRs were analyzed when the number of single-RT-qPCR was between 80 and 120% of the expected number, according to the reported pool-size (n=470 independent pool-RT-qPCRs). Horizontal lines represent the means of the fractions stratified by calendar week. **c**, Categorization of number of positive single-RT-qPCRs/positive pool-RT-qPCR stratified by calendar week.

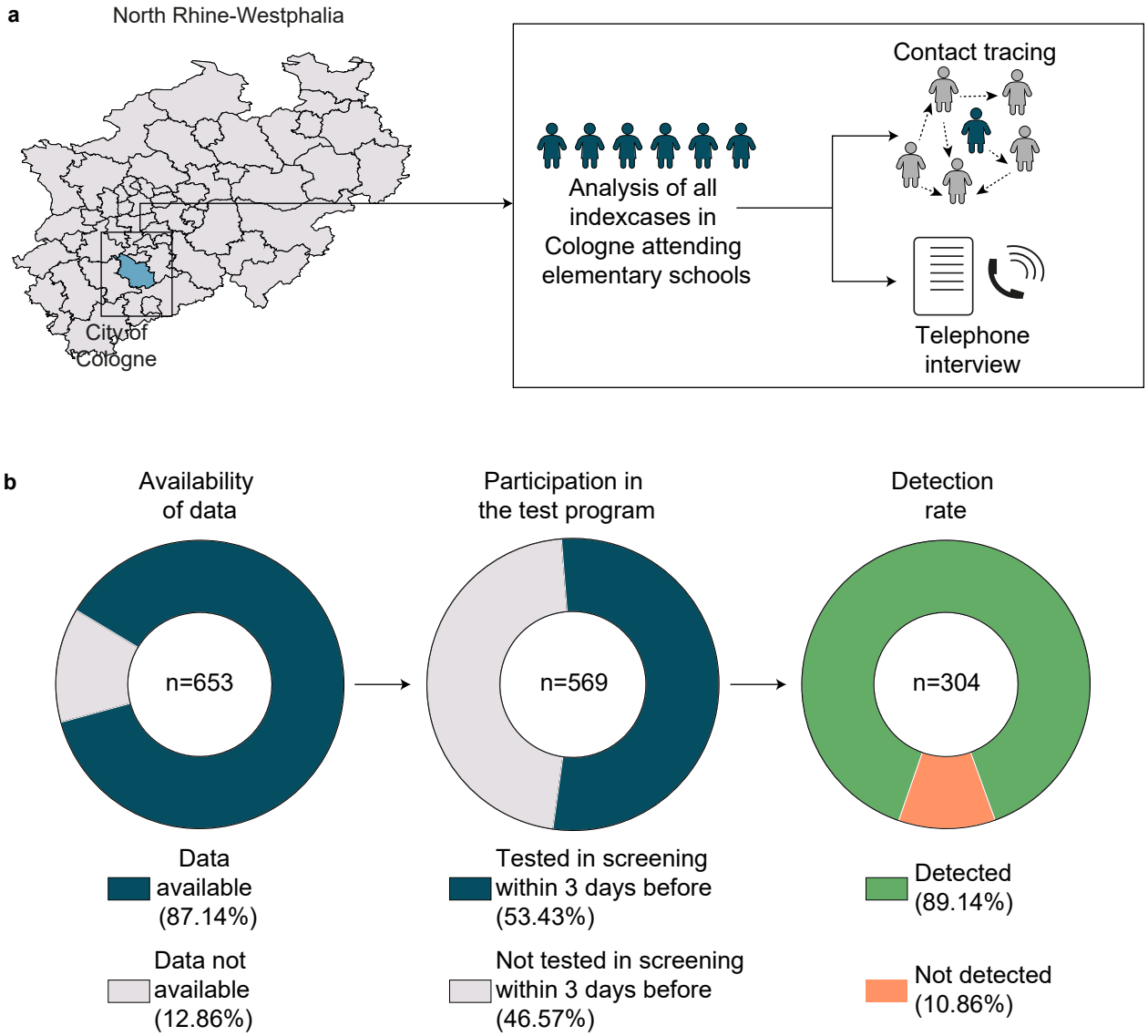

Supplementary Fig. 7: Determination of the SARS-CoV-2 detection rate of the Lolli-Method
a, Contact-tracing data of all index-cases attending elementary schools in the city of Cologne were analyzed.
b, Pie-chart categorizing all index-cases attending elementary schools in Cologne.

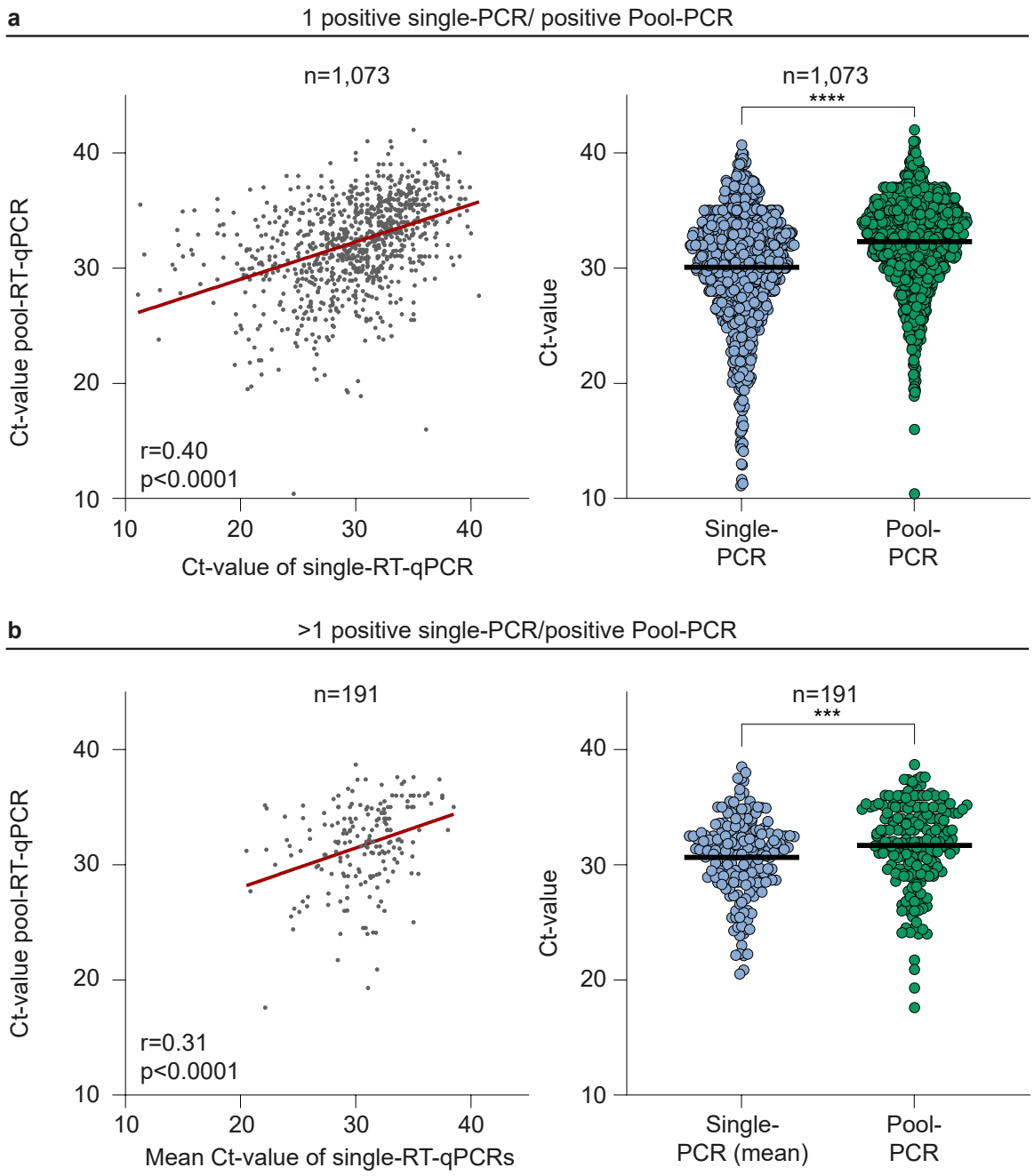

Supplementary Fig. 8: Correlation between Ct-values of pool-RT-qPCR and matched single-RT-qPCRs.

a, Left: Spearman correlation (two-tailed) of Ct-values of pool-RT-qPCRs containing only one positive single-RT-qPCR and the Ct-value of their matched single-RT-qPCR (n=1,073; r=0.4; p<0.0001). Right: Single- and pool-RT-qPCRs are plotted by Ct-value. Horizontal lines indicate mean Ct-values (p<0.0001, two-tailed WSR).**b**, Left: Spearman correlation (two-tailed) of Ct-values of pool-RT-qPCRs containing more than one positive single-RT-qPCR and the mean Ct-value of their matched single-RT-qPCRs (n=191; r=0.31, p<0,0001). Right: Single- and pool-RT-qPCRs are plotted by Ct-value/mean Ct-values. Horizontal lines indicate average Ct-values (p=0.0004, two-tailed WSR).

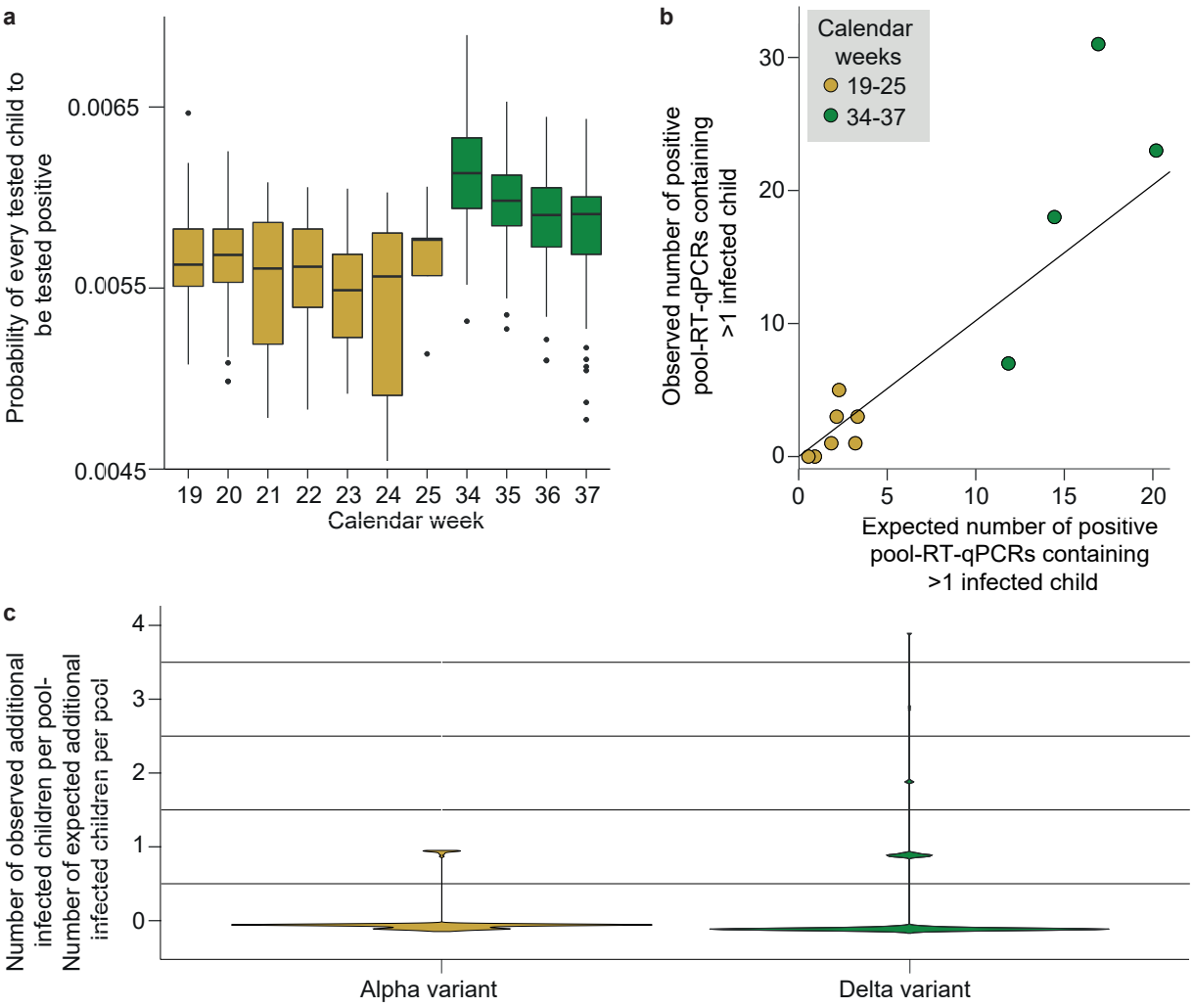

Supplementary Fig. 9: Modelling differences in infections dynamics of SARS-CoV-2 variants with the Lolli-Method in schools

a, Boxplot indicating the probability of every child to be tested positive stratified by calendar week. N=782 biologically independent positive pool-RT-qPCRs. Calendar weeks 19-25 (yellow boxes) und 34-37 (green boxes) are included in this plot. The horizontal lines indicate the medians, the lines at the top and at the bottom of the boxes indicate first and third quartiles, the vertical bars represent upper and lower whiskers and the dots represent outliers. **b**, Observed number stratified by expected number of positive pool-RT-qPCRs containing >1 infected child per calendar week. Calendar weeks 19-25 (yellow dots) and 34-37 (green dots) are included in this plot. **c**, Violin plot indicating the difference between observed and expected number of additional infected children per positive pool-RT-qPCR stratified by SARS-CoV-2 variant (p=0.002, WSR).

Supplementary Table 1

SEIR-model parameter description

Parameter	Description	Value	Reference
τ_{pre}	Time between infection and infectiousness	3 days	*40*
τ_{inf}	Duration of infectiousness	6 days	*41*
R0	Basic reproduction number	2,5	*42*
		4,5	*43,44*
		7,5	*37*
p_{in}		0,10%	*Assumption*
		0,01%	
p_{PCR}	False-negative rate of RT-qPCR	2,00%	*45,46,47*
g	Exponential growth rate of viral load	1/(4,5 days)	*48*

Supplementary Table 2

Tested schools and students

District	Schools (n)			Students (n)		
	Elementary schools	Schools for special needs	Other schools	Elementary schools	Schools for special needs	Other schools
Aachen	99	22	0	18629	3358	0
Bielefeld	51	13	0	12475	2292	0
Bochum	52	14	0	11584	3310	0
Bonn	55	8	1	12230	1352	416
Borken	74	11	0	14483	1598	0
Bottrop	20	3	0	4010	224	0
Coesfeld	40	5	0	8182	860	0
Dortmund	91	19	1	21496	2868	738
Duisburg	77	15	0	18417	2607	0
Düren	55	7	1	9272	1385	481
Düsseldorf	94	17	0	21777	3178	0
Ennepe-Ruhr-Kreis	56	8	1	10709	1340	375
Essen	87	22	0	20396	3865	0
Euskirchen	39	9	0	6729	1206	0
Gelsenkirchen	41	10	0	10411	1953	0
Gütersloh	69	15	0	13840	1809	0
Hagen	33	6	0	7186	1160	0
Hamm	28	6	1	6682	797	344
Heinsberg	55	7	0	9085	974	0
Herford	51	6	0	9230	1046	0
Herne	21	6	1	5593	656	1065
Hochsauerlandkreis	64	12	0	8756	1038	0
Höxter	25	6	0	4841	621	0
Kleve	58	11	0	11105	1513	0
Krefeld	34	8	1	7955	1459	487
Köln	159	28	0	38152	4844	0
Leverkusen	25	4	0	6457	399	0
Lippe	66	13	0	13229	1850	0
Mettmann	83	14	0	17856	1841	0
Minden-Lübbecke	64	14	2	11554	1477	998
Märkischer Kreis	70	11	1	14360	1822	518
Mönchengladbach	43	12	0	9408	1680	0
Mülheim an der Ruhr	24	4	0	6100	1067	0
Münster	47	8	2	9956	1798	516
Oberbergischer Kreis	51	11	0	10204	1783	0
Oberhausen	31	5	0	7202	715	0
Olpe	35	7	0	4885	1022	0
Paderborn	64	10	0	11768	1834	0
Recklinghausen	99	20	0	21906	3170	0
Remscheid	21	6	0	3976	509	0
Rhein-Erft-Kreis	78	15	0	17877	2135	0
Rhein-Kreis Neuss	79	9	0	17238	1400	0
Rhein-Sieg-Kreis	102	24	0	22715	3137	0
Rheinisch-Bergischer Kreis	56	8	0	10376	1165	0
Siegen-Wittgenstein	62	8	1	9868	875	333
Soest	58	13	1	10648	1862	280
Solingen	27	6	0	5608	622	0
Steinfurt	89	17	1	16816	2154	103
Unna	63	8	0	13860	1211	0
Viersen	48	8	1	10105	966	336
Warendorf	58	5	0	10431	768	0
Wesel	77	12	0	15722	2525	0
Wuppertal	57	11	2	13085	1558	688
Total	3105	577	18	646435	88658	7678

Supplementary Table 3

Equipment for SARS-CoV-2 screening in schools

Lab ID	RNA extraction	RT-qPCR equipment
1	1. Echolution Viral RNA/DNA Swab Kit (Bio Echo Life Science GmbH)	1. 2019-nCoV: RT-PCR Kit (BGI) 2. ABI 7500 / ABI 7500-fast / ABI 7300 (Applied Biosystems)
2	1. KingFisher Flex (ThermoFisher) 2. Tecan Freedom EVO-2 100 Base (Tecan) 3. Quick-DNA/RNA Viral MagBead (Zymo)	1. ViroQ Rapid SARS-CoV-2 (BAG Diagnostics) 2. CFX96 (BioRad)
3	Not available	1. LightCycler® 480 II (Roche Diagnostics)
4	1. Chemagen 360 (Perkin Elmer)	1. Cobas 480 Z II (Roche Diagnostics) 2. QuantStudio 5 (Thermofisher) 3. QuantStudio 7pro (Thermofisher)
5	1. Chemagen 360 (Perkin Elmer)	1. Hologic Panther Aptima Sars Co-V-2 Assay (Hologic) 2. Thermos TaqPath Covid-19 Kit (Thermofisher) 3. CFX 96 (BioRad) 4. CFX 384 (BioRad)
6	1. KingFisher (ThermoFisher)	1. Allplex™ SARS-CoV-2 Master Assay (Seegene)
7	1. KingFisher Flex (FA ThermoFisher) 2. Maelstrom 9600 (Tanbead) 3. RNA Extraction Kit AE1 (GSD NovaPrime®)	1. AriaDx (Agilent Technologies) 2. ABI 7500 FAST (FA ThermoFisher) 3. SARS-CoV-2 RT-PCR (GSD NovaPrime®)
8	1. Roche SARS-CoV-2 KIT (Roche Diagnostics) 2. AltoStar AM 16 (Altona Diganostics)	1. Cobas 6800 (Roche Diagnostics) 2. CFX 96 (BioRad)
9	Not available	Not available
10	1. Maelstrom 9600 (TanBead)	1. Allplex™ SARS-CoV-2 Master Assay (Seegene)
11	1. RoboPrep 96 (Biotecon Diagnostics)	1. CFX DX (BioRad) 2. LightCycler® 480 II (Roche Diagnostics)
12	1. Roche SARS-CoV-2 KIT (Roche Diagnostics) 2. KingFisher Flex (ThermoFisher) 3. ExtraStar 1.0, (Altona Diganostics)	1. Cobas 6800 (Roche Diagnostics) 2. Cobas 8800 (Roche Diagnostics) 3. CFX96 (BioRad) 4. RealStar SARS-CoV-2 RT-PCR Kit, (Altona Diganostics)

Description of additional Supplementary Files

File Name: Supplementary Data 1
Description: Validation of the Lolli Method (Morning and during the day)

File Name: Supplementary Data 2
Description: Validation of the Lolli Method (Before and 1 hour after breakfast)

File Name: Supplementary Data 3
Description: Validation of the Lolli Method (Different swab-types)

File Name: Supplementary Data 4
Description: Validation of the Lolli Method (Pooling)

File Name: Supplementary Data 5
Description: Validation of the Lolli Method (Specificity)

File Name: Supplementary Data 6
Description: Overview on SARS-CoV-2 screening in schools

File Name: Supplementary Data 7
Description: Code of the SEIR-model

File Name: Supplementary Data 8
Description: Code of the statistical modelling